Which visual working memory model accounts best for target representation in the attentional blink?

Shuyao Wang[1], Aytaç Karabay[1,2], Elkan G. Akyürek[1]

[1] Department of Psychology, Experimental Psychology, University of Groningen, Groningen, The Netherlands

[2] Department of Psychology, New York University Abu Dhabi, Abu Dhabi, UAE

Author Note

Word count: 12650

Keywords: Working memory; Attentional blink; Model comparison; Continuous report

The authors declare that they have no conflict of interest.

Correspondence concerning this article should be addressed to Shuyao Wang, Department of Psychology, Experimental Psychology, University of Groningen, Grote Kruisstraat 2/1, 9712 TS Groningen, the Netherlands. Email: shuyao.wang@rug.nl

Abstract

The nature of working memory (WM) limitations has been a topic of long-standing debate, with several models proposed to elucidate this issue. In this study, we conducted a systematic comparison of eight visual WM models to assess their ability to account for target consolidation during the attentional blink (AB). The AB phenomenon refers to where participants often fail to detect and/or encode the second of two targets when there is a short time interval of ~500 msec or less between them, providing a valuable tool for investigating WM limitations. Despite the growing consensus on the applicability of some WM models, such as the standard mixture model and the variable precision model, to the AB domain, no study has systematically evaluated these models in this context. We addressed this gap by comparing the performance of eight widely adopted visual WM models in four different AB datasets, drawn from three separate laboratories. We fitted each model and computed the Akaike Information Criterion (AIC) values at an individual level, across different conditions and experiments, based on which we compared the models by their average relative AIC values and model ranks. We found that most models, excluding the variable precision model, fit well to AB datasets. We nevertheless also observed that experimental properties, such as the choice of stimuli or the spatial arrangement of targets, can result in different model rankings. Our results can help researchers to select the best model for their AB studies, and thereby gain a better understanding of their data.

1. Introduction

Visual working memory (WM) plays a pivotal role in information processing, yet it is challenging to encode all information completely. A substantial amount of research has focused on investigating the limitations of WM, which include storage limitations – the capacity of how many items can be encoded (Cowan, 2001; Miller, 1956; Pashler, 1988); but also processing limitations – the difficulties faced when processing and consolidating multiple items that appear either concurrently or in a rapid succession (Jolicœur & Dell'Acqua, 1998; Ricker & Cowan, 2014).

In exploring the processing limitations of WM, the attentional blink (AB) phenomenon in particular has emerged as a valuable paradigm, offering unique insights into how our cognitive system handles rapidly presented information (Akyürek et al., 2007; Jolicœur & Dell'Acqua, 1998; Ricker & Hardman, 2017; Vogel & Luck, 2002). The AB refers to the failure to identify the second (T2) of two briefly presented target stimuli, when the time interval (or lag) between them is within 200 – 500 msec (Broadbent & Broadbent, 1987; Raymond et al., 1992). In the field of AB research, categorical items such as letters, numbers, or images have traditionally been utilized in the rapid serial visual presentation (RSVP) paradigm (for a review, see Dux & Marois, 2009; Martens & Wyble, 2010).

While this typical paradigm has proven to be an effective method for studying the AB itself, it presents inherent challenges in evaluating the quality of target representations maintained in WM during the AB window. In response to this challenge, recent studies have incorporated the continuous report task into the RSVP paradigm, as is also frequently utilized in the visual WM field (Bays et al., 2009; Fougnie & Alvarez, 2011; Kool et al., 2014; Oberauer et al., 2017; Zhang & Luck, 2008). During the task, participants are required to memorize targeted visual items, which are identified by a basic visual property that varies on a continuous, usually circular, dimension, such as color or orientation. In the reproduction

stage, participants are then asked to recall the target on a continuous response scale, such as recreating its orientation by rotating a Gabor (Wilken & Ma, 2004). Consequently, the performance of a continuous report task is not measured in a binary format, but rather as the divergence between the target value and the corresponding response. This approach makes it possible to quantify the target representations stored in WM.

It is known from WM research that observers' error distributions derived from continuous reproduction data typically have a 'long tail' (Wilken & Ma, 2004; Zhang & Luck, 2008), giving rise to a debate surrounding the interpretation of this "guessing behavior". One side holds the view that WM is comprised of a fixed, limited number of discrete "slots" dedicated to item storage, with large memory errors (e.g., those far away from the target value) occurring when items are not stored in WM, reflecting pure guessing (Alvarez & Cavanagh, 2004; Bays et al., 2009; Zhang & Luck, 2008). Several models of WM feature this discrete slot structure, including the standard mixture, slot and slots plus resource models (Zhang & Luck, 2008). The other side hypothesizes that WM is a continuous resource that can be distributed freely over items. According to this view, large memory errors arise when items are encoded with extremely low precision as opposed to high precision (Brady & Alvarez, 2011; Fougnie et al., 2012; van den Berg et al., 2012). The variable precision model and its variants implement this continuous resource view (Fougnie et al., 2012; van den Berg et al., 2012)).

A recently proposed model, the target confusability competition (TCC) model, offers a third perspective on the continuous reproduction task in the context of visual WM (Schurgin et al., 2020). The TCC model posits that memory errors, regardless of their magnitude, arise from a single process. Specifically, it suggests that the activation of target features is based on a psychophysical scaling function. This function represents the similarity between features, which is determined by their non-linear distance on the circular scale and can be effectively

estimated through an independent perceptual comparison experiment. The TCC model then integrates this psychophysical scaling function into a signal-detection framework, providing a new understanding of errors in WM.

The integration of the continuous report task into the traditional AB paradigm creates opportunities for utilizing these working memory models to quantitatively assess memory performance during the AB task. Previously, Asplund et al. (2014) applied a mixture-model analysis (Zhang & Luck, 2008) to data obtained by explicitly asking participants to recall their perception of T2 along a continuous circular dimension. Through this approach, the authors were able to quantify the precision of T2 representations and the proportion of guess responses for T2. Their findings indicated that AB affects T2 perception in an all-or-none manner, with an increased percentage of random guess trials at shorter lags, while lag had no effect on T2 precision.

In a similar vein, Karabay et al. (2022) employed hierarchical Bayesian estimation to explore the variability in the precision and guess rate parameters of the standard mixture model at different time intervals between two targets. Their study showed that T2 awareness during the AB can be both gradual and discrete. Specifically, when the identification of the first target (T1) required the focus of attention on a single spatial location, T2 awareness was discrete, with the guess rate varying significantly; on the contrary, when T1 identification induced a spatial spread of attention, T2 awareness was gradual, with variations in precision. Sy et al. (2021) utilized both the standard mixture and variable precision models, and also found that the temporal loss of T2 information during the AB might be either gradual or discrete. Specifically, when two targets (T1 and T2) shared a visual feature, their results indicated a gradual loss of T2 precision, with the variable precision model providing a better fit to the data. In contrast, they observed a discrete loss of T2 information when participants had to switch their attention to different target features (i.e., color for T1 and orientation for

T2), and in this case the mixture model performed better than the variable precision model in terms of fitting the data. While the primary objective of Sy et al. was to discern whether perception during the attentional blink is discrete or graded, it is worth noting that their results present mixed results in terms of model performance.

The mixed performance of working memory models in AB tasks, along with their fundamental theoretical divergences, highlight the need for a systematic investigation of these models within the AB context. Current literature is limited, with comparisons mainly focusing on the standard mixture and variable precision models, while neglecting other vital models. For example, the ensemble integration model (Brady & Alvarez, 2011) assumes that other non-target items impact the report of a specific target item. In the context of the AB, this hypothesis is supported by Akyürek and Hommel (2005; Akyürek et al., 2012), who discovered that temporal integration occurs with successive targets in RSVP.

Our study aims to provide the first systematical comparison between the eight commonly used visual WM models in the AB domain: the standard mixture model, the slot model, the slots plus resource model, the swap model, the ensemble integration model, two versions of the variable precision model and the TCC model. These models fundamentally diverge in how they interpret memory errors in the continuous reproduction task. Our objective is to determine which model(s) provide the most accurate and comprehensive explanation of the empirical data underlying the AB phenomenon. To ensure the generalizability and robustness of our results, we analyzed continuous report data from three previously conducted AB studies by distinct research groups (Asplund et al., 2014; Karabay et al., 2022; Tang et al., 2020), in conjunction with data from a new experiment we have undertaken. By doing so, our study aims to offer insights that contribute to both the fields of WM and AB research.

2. Method

2.1. Model Details

Slot model family: Models with limited number of WM slots.

The family of slot models, including the standard mixture, slot and slots plus resource models is built upon the core assumption that WM consists of a limited number of discrete slots for storing visual representations (Cowan, 2001; Luck & Vogel, 1997). If the target object has been stored in one of these slots, its information is maintained in WM. In contrast, if the item has not been stored in any of these slots, then no information about it remains in WM.

Standard mixture model (StM). The StM model (Zhang & Luck, 2008) proposes a mixture distribution for responses. When items are successfully stored into WM, the corresponding response values tend to cluster around the actual value, thereby forming a Von Mises distribution. Conversely, when item information is not available in WM, the reported values are expected to be random, conforming to a uniform distribution. The probability of this guessing is denoted by the height of this uniform distribution. Taken together, the response error distribution in the StM model is given by:

$$p(x|s, g, sd) = (1 - g)VM\big(x - s; 0, k(sd)\big) + g\,\frac{1}{2\pi},$$

where x is the reported value, s is the target value. The model parameter g, or the guess rate, indicates the proportion of trials where subjects are presumed to make random guesses. The von Mises distribution is expressed as:

$$VM(x - s; 0, \kappa) = \frac{1}{2\pi I_0(\kappa)} e^{\kappa \cos(x - s)}$$

In this formula, κ, the concentration parameter of the Von Mises distribution, signifies the precision of memory representations. It is analogous to the standard deviation sd in the

normal distribution. $I_0(\kappa)$ is the modified Bessel function of the first kind of order 0, which ensures that the total probability density integrates to 1.

Slot model. The Slot model (Cowan, 2001; Luck & Vogel, 1997), which serves as the classic representation of this family, posits that there is a fixed number of storage slots in WM. When the number of items to be remembered, known as the set size, exceeds the maximum number of available slots, any excess items are disregarded. Consequently, in the Slot model, the guess rate (g) is correlated with the maximum number of slots. The response error distribution is formally given by:

$$p(x|s, g, sd) = (1 - g)VM\big(x - s; 0, \kappa(sd)\big) + g\frac{1}{2\pi},$$

The guess rate g depends on the model parameter, *capacity* (*K*), according to the following relationship. When $K \geq N$ (set size), all items can be remembered, and the guess rate would equal zero. When $K < N$:

$$g = 1 - \frac{K}{N}.$$

Slots plus resource model (SR). The SR model (Awh et al., 2007; Zhang & Luck, 2008), like previous models, hypothesized a fixed, finite capacity of WM wherein a certain number of items can be stored. What distinguishes the SR model is its unique approach to WM resource allocation. Specifically, most WM resources are preferentially assigned to a probed item, with only a minimal amount for other items that are considered less relevant. The SR model proposes that when the number of items is fewer than the slots available, the surplus resources improve the precision of the stored items. In such instances, we anticipate significant variance in the precision (standard deviation, *sd*) of WM, depending on the set size. Formally, the response error distribution is given by:

$$p(x|s, g, sd) = (1 - g)VM\big(x - s; 0, \kappa(sd)\big) + g\frac{1}{2\pi}.$$

Here, the *sd* is extrapolated using the SR model's parameters, *bestSD* and the number of probed items *n*, as follows:

$$sd = bestSD \times n^2,$$

where $bestSD$ denotes the precision when all WM resources are used for storing a single item, and n is the number of items that can be stored in WM, depending on the *capacity K* and set size N:

$$n = \min(capacity\ K, set\ size\ N).$$

The guess rate is linked to the *capacity K* in the same way as in the Slot model.

The variable precision models: Models that assume WM consists of a resource pool.

The variable precision models (Fougnie et al., 2012; van den Berg et al., 2012) propose that WM resources are allocated to items in a continuous and variable manner, which causes the precision of WM representation to vary across items and trials. Although the variable precision models and the SR model both suggest that WM is not (entirely) quantized, there are two primary distinctions between them. First, the variable precision models define WM limitations by the quality of the representation, as opposed to the number of items memorized. This is in contrast to the SR model, which puts emphasis on the item count. Second, the variable precision models imply a variability of WM resources across trials and items. The SR model, in contrast, implies an equal level of precision across all items and trials, when the set size is fixed.

Variable precision model (VP). In the VP model proposed by van den Berg et al. (2012), item information does not undergo a total loss. Instead, the quality of the item representation may severely degrade, resulting in extremely low precision. Therefore, the response error distribution is given by:

$$p(x|s, J) = VM(x - s; 0, \kappa(J)).$$

Here, each item is encoded with precision J, which is defined as the Fisher information. The concentration parameter κ is related to J through the following relationship:

$$J = \kappa \frac{I_1(\kappa)}{I_0(\kappa)},$$

where I_0 represents the modified Bessel function of order zero and I_1 represents the modified Bessel function of order one.

The core hypothesis in the VP model is that the precision J varies independently across items and trials. Furthermore, the precision J itself follows a specific distribution as a random variable. Van den Berg et al. (2012) further assume this specific distribution of precision J to be Gamma with mean precision $\bar{J}$ and scale parameter τ:

$$p(J|\bar{J};\tau) = Gamma(J|\bar{J};\tau).$$

Therefore, the response error distribution of the VP model is a mixture of an infinite set of Von Mises distributions:

$$p(x|s;\bar{J},\tau) = \int VM((x-s;0,\kappa(J))Gamma(J|\bar{J};\tau)\,dJ$$

Variable precision model with guess rate (VPG). In the current study, we also employed another version of the VP model with an extra *guess rate* parameter (Fougnie et al., 2012). Mathematically, the response distribution is then given by:

$$p(x|s,g,mo,sd) = (1-g)\int VM((x-s;0,\kappa(J))Gamma(J|mo;sd)\,dJ + g\frac{1}{2\pi}.$$

Thus, the VPG model has three free parameters: guess rate (g), the mode (*mo*) and the standard deviation (*sd*) of the Gamma distribution of precision J.

Interference models: Models that assume there are interaction between items.

Ensemble integration model (EnsInt). The aforementioned models suggest that each item is stored in WM independently, which implies there is no interaction between these items. However, Brady and Alvarez (2011) demonstrated that the representation in WM is not only affected by the item itself, but also by the integration of information of all the stimuli that are displayed. Their results showed that the reported size of a target item was shifted toward the mean size of the items with the same color, as well as the mean size of all items displayed. The EnsInt model implemented in the current study is a simplified version of the

Brady & Alvarez (2011) model, which introduces a parameter that represents the bias towards the mean value of all distractors. Since the first target is the only other relevant item in typical continuous-report AB tasks, we used T1's value for this parameter, slightly simplifying the model. Formally, the error distribution of the EnsInt model is given by:

$$p(x|\mu_s, g, sd) = (1-g)VM\big(x-\mu_s; 0, \kappa(sd)\big) + g\,\frac{1}{2\pi},$$

where μ_s refers to the biased mean value, which is estimated based on the differences between the target (T2) and the other item (T1).

Swap model. This model can be considered as an extension of the StM model. In addition to the two components of the response error distribution, namely a uniform distribution that indicates the proportion of random-guessing trials and a Von Mises distribution that represents the memory precision, Bays et al. (2009) introduced a third source of error: The probability of incorrectly reporting non-target items. Consequently, the Swap model has a three-component structure, including precision, guess rate, and swap rate (estimated by the measurement of the distance between reported values and non-target items):

$$p(x|s, g, sd, \beta) = (1-g-\beta)VM\big(x-s; 0, \kappa(sd)\big)$$

$$+\beta\,\frac{1}{m}\sum_{i}^{m} VM(x-\theta_i; 0, \kappa(sd)) + g\,\frac{1}{2\pi}$$

where β, the swap rate, denotes the probability of incorrectly reporting the non-target items (distractors, i.e., T1) and where $\{\theta_1, \theta_2, \ldots \theta_m\}$ are the values of a set of m distractors.

Signal-detection model: Target confusability competition model (TCC). The TCC model posits that memory representations can be characterized using a single parameter known as the memory strength (d', Schurgin et al., 2020). The cornerstone of the TCC model lies in its integration of the psychophysical similarity function and signal detection theory. The initial stage of the TCC model involves quantifying the psychophysical similarity within a given feature space (e.g., color), elucidating how familiarity propagates within that specific

stimulus field. Subsequently, the model applies signal detection theory to introduce noise into the assessed similarity space.

To illuminate this model's mechanics, consider a single continuous report trial where the task is to recall a specific color (e.g., 'purple') using a color wheel. Upon encoding 'purple' into our working memory with a memory strength of $d' = 3$, the familiarity of 'purple' and other colors on the color wheel increases in accordance with the psychophysical similarity ($d_x = d' f(x)$). Following this, noise is introduced into each color representation. The ultimate memory signal then becomes this familiarity distorted by noise. The color reported will be the one that exhibits the highest signal.

2.2. Datasets

As summarized in Table 1, we obtained three existing datasets from three separate laboratories (Asplund et al., 2014; Karabay et al., 2022; Tang et al., 2020), and added a fourth, new dataset in the present paper (Wang et al.).

Asplund et al. (2014). The first dataset was obtained from Experiment 1 in Asplund et al. (2014), where square-shaped targets were embedded in circle-shaped colored distractors. T1 was filled with either black or white, while the T2 color was randomly chosen from 180 equiluminant colors. T2 appeared at the first, second, fourth, or eighth position (labeled as Lag 1, Lag 2, Lag 4, and Lag 8) following T1. The stimulus duration for each participant was set by a staircase method and resulted in an average value of 150 ms (*SD* = 10 ms). At the end of the stimulus stream, participants were asked to reproduce T2 using a color wheel, and to report whether the first target was black or white.

Tang et al. (2020). The second dataset was retrieved from two behavioral experiments in the AB study by Tang et al. (2020), where a RSVP task was again employed. Specifically, there were 20 Gabor patches, and the orientation of the Gabors were integer angles ranging from 0 to 179 degrees, without replacement. Participants were instructed to memorize two

targets (high-frequency Gabors) among distractors (low-frequency Gabors) and reproduce them at the end of each trial. Each target or distractor appeared for 40 ms, and the next item followed after a blank interval of 80 ms. The time interval between two targets was manipulated by presenting different numbers of distractors in-between (lag). In Experiment 1, there were five lag conditions (1, 2, 3, 5, 7), while in Experiment 2, there were two lag conditions (3, 7).

Karabay et al. (2022). Karabay et al. (2022) used two different paradigms, dwell time (DT) and RSVP, both with continuous report tasks, to examine the nature of awareness in the AB. We acquired seven datasets from their experiments. Experiment 1A, 1B, 2A, and 2B were run with the DT paradigm. Both targets were orientation gratings (in Experiment 1A and 1B) or colors (in Experiment 2A and 2B). T1 and a distractor were presented, at the same time, above or below the fixation dot, at an equal distance. The display of T2 was the same as T1, except the location changed to the left or right side of the fixation dot. On each trial, T1 and T2 target arrays were followed by a mask. The stimulus-onset asynchrony (SOA) between T1 and T2 was set to 250 ms and 800 ms. The RSVP paradigm was used in Experiment 3, 4, and 5, in which the targets were always orientation gratings. The number of distractor items between two targets was 2 (Lag 3, 300 ms SOA) or 7 (Lag 8, 800 ms SOA). In Experiment 3, the two targets appeared among a stream of distractors, similar to the design in Tang et al. (2020). In Experiment 4, there were simultaneously two streams of stimuli at the left and right sides of the fixation dot. In Experiment 5, T1 was presented within a single stream of distractors, but split into a dual stream with the presentation of T2, as in Experiment 4.

Table 1

Details of the data sets.

Datasets	Exp	SOA (ms)	Lag	T1 feature	T2 feature	Original subject number	Subject number for the analysis
Asplund et al., 2014	Exp 1	NA	1, 2, 4, 8	Categorical	Color (1°-180°)	27	21
Tang et al., 2012	Exp 1	50, 240, 360, 600, 720	1, 2, 3, 5, 7	Orient. (1°-180°)	Orient. (1°-180°)	22	22
	Exp 2	360, 720	3, 7	Orient. (1°-180°)	Orient. (1°-180°)	22	22
Karabay et al., 2022	Exp 1A	250, 800	NA	Orient. (1°-180°)	Orient. (1°-180°)	23	22
	Exp 1B	250, 800	NA	Orient. (1°-180°)	Orient. (1°-180°)	21	21
	Exp 2A	250, 800	NA	Color (1°-360°)	Color (1°-360°)	26	24
	Exp 2B	250, 800	NA	Color (1°-360°)	Color (1°-360°)	27	23
	Exp 3	300, 800	3, 8	Orient. (1°-180°)	Orient. (1°-180°)	24	23
	Exp 4	300, 800	3, 8	Orient. (1°-180°)	Orient. (1°-180°)	24	22
	Exp 5	300, 800	3, 8	Orient. (1°-180°)	Orient. (1°-180°)	23	23
Wang et al. data	Exp 1	90, 300, 800	1, 3, 8	Orient. (1°-180°) or Color (1°-360°)	Orient. (1°-180°) or Color (1°-360°)	28	22

Note. Exp = Experiment; Orient. = Orientation; Wang et al. data refers to the new dataset collected in the present study.

2.3. Wang et al. data

In the new experiment, we manipulated feature changes between targets in the AB task (same or different), hypothesizing that matching target features might cause mutual bias in target reports, which might affect the model selection. Like the other studies, this experiment also featured continuous report of targets.

2.3.1. Participants

The minimum sample size of 24 subjects was determined by means of a G-power analysis (Faul et al., 2007), with the following parameters: significance level (α = .05), beta-level (β = .2), and a medium to large effect size (Cohen's d_z = .6). Twenty-eight undergraduate students (seventeen females and eleven males) from the University of Groningen were recruited in exchange for course credits (mean age = 19.6, range = 18-27). All participants reported normal or corrected-to-normal visual acuity and no color blindness. Informed consent forms and instructions were given to the participants prior to participation. Nine participants were excluded from further analysis, based on our exclusion criteria (see *2.8. Subject exclusion*). Prior to its execution, ethical approval was obtained from the ethical committee of the Psychology Department of the University of Groningen (Approval code PSY-1819-S-0209). The study was conducted in accordance with the Declaration of Helsinki (2008).

2.3.2. Apparatus and stimuli

Participants were individually seated on a desk chair in sound-attenuated lab chambers, at a viewing distance of approximately 60cm from a 22" CRT monitor (Iiyama MA203DT). The screen was set at a 1280 x 1024-pixel resolution, 16-bit color depth, and a 100Hz refresh rate. The trials were prepared and run in OpenSesame 3.2 (Mathôt et al., 2012) with the PsychoPy back-end (Peirce, 2007; 2009), under the Microsoft Windows 7 operating system. All the stimuli were displayed in the center of the screen on a grey background (RGB: 128,128,128), as shown in Figure 1A. There were two kinds of target stimuli in the RSVP stream (Figure 1B). The first kind of target consisted of orientation gratings with a spatial frequency of 1.8 cycles/degree of visual angle, presented within a circle of 2.2° of visual angle. The orientation of the gratings was chosen randomly from the range of 0°-179°. The other kind of target consisted of circles (2.2° of visual angle) filled with one of 360 colors,

which were chosen randomly from the HSL color spectrum. The distractors were grey-scale mosaic images (2.2° × 2.2° of visual angle), retrieved from Karabay et al. (2022).

2.3.3. Procedure

A 2 (Target feature: same or different) x 3 (Lag: 1, 3, 8) factorial design was implemented in this experiment. Two practice blocks, each including 16 trials, were administered at the beginning, which were excluded from the analysis. After that, there were 540 experimental trials evenly distributed into 15 blocks. Each trial started with a fixation dot that randomly lasted for 600-800ms. There were 18 items within the RSVP stream. Each item was shown for 80 ms, separated by a 10 ms inter-stimulus interval (ISI). T1 was randomly presented at the fifth, sixth, or seventh position of the stream. T2 was presented consecutively (Lag 1), after two items (Lag 3), or after seven items (Lag 8), following T1. T1 and T2 could have either the same feature (color or orientation), or different features. At the end of the stream, after a blank interval of 500ms, two response prompts were displayed successively.

Participants were asked to reproduce the two targets in the correct order. They were asked to reproduce the target orientation by rotating a probe grating, or to reproduce the target color by choosing the exact color from a color wheel. Responses were collected with a standard mouse. Trial-based feedback was provided only in practice trials: A happy smiley was shown for correct trials, and an unhappy smiley for incorrect trials. Responses close to target values (below 22.5° reproduction error) were considered correct responses for feedback. In the experimental blocks, the average performance on T1 and T2 were displayed at the end of each block. During the experiment, participants could have a self-paced break between blocks. The whole session took about 90 minutes to complete.

Figure 1

Illustration of the design of the newly conducted experiment.

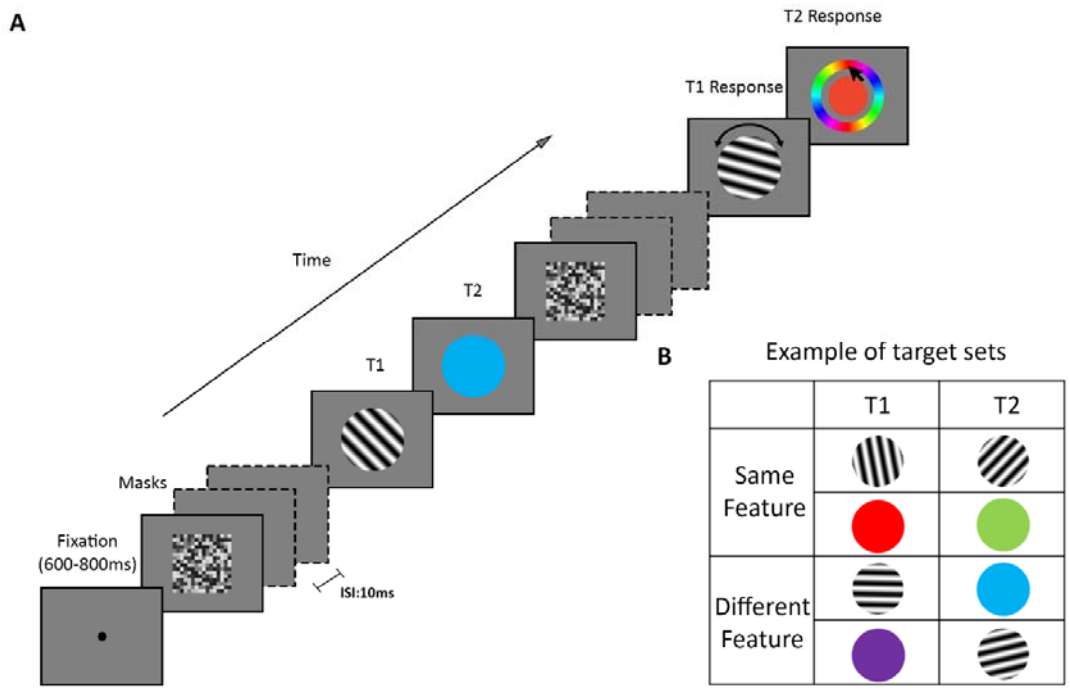

Note. (**A**) An example trial of the dual-target RSVP task at Lag 3. In this instance, the two targets have different features. (**B**) Examples of possible targets in all combinations and orders of the two targets.

2.4. Data Preparation

As indicated, all the data sets we gathered for analysis were obtained from continuous-report AB tasks. We reorganized the datasets to form a uniform structure, as per the following procedure:

1. For each trial, response error for each target (T1 and T2) was calculated by subtracting the response value from the actual one.
2. Trials in which the absolute deviations between T1 and T2 values were less than 22.5 degrees were discarded.
3. Response errors were limited to a range from -90° to 90° for orientations and from -180 to 180 for colors.

4. Performance of T2 was evaluated in two distinct conditions:
    a. T1 correct Condition (T2|T1) – This condition is often employed in AB studies. In this condition, we included only the trials in which the absolute error of T1 was less than or equal to 22.5 degrees for orientations (45 degrees for colors).
    b. T1 incorrect condition – This condition included the trials in which the absolute error of T1 exceeded 22.5 degrees for orientations (45 degrees for colors).

Given that the set size remained constant across all our data sets, we took into account that some models (e.g., the SR model) incorporate set size for parameter estimation. Hence, we also analyzed T2 performance when T1 was reported incorrectly, as this represents a scenario where the set size equals one. Although this condition does not strictly correspond to a true single set size condition, it does provide a valuable approximation of model performance when the memory load is set to one, while the typical T2|T1 performance analysis evaluates the models' performance when the memory load is two.

2.5. Model fitting

We employed maximum likelihood estimation (MLE) as our chosen approach to fit all of the aforementioned models to our data sets. The general logic of MLE is to maximize the likelihood function to find the specific parameter value, with which the chosen probabilistic model is most "likely" to generate the observed data. Specifically, for each subject and condition within a single experiment, we carried out model fitting using the built-in MLE function in MemToolbox (Suchow et al., 2013). This allows us to obtain the best estimates of the model parameters at the individual level (See Supplementary Materials A for details of parameter estimates).

2.6. Model comparison

In terms of model comparison and selection, it is important to strike a balance between model flexibility and overfitting. Although flexible models can accommodate a wide range of datasets by introducing additional parameters, they may lack supporting evidence and can lead to overfitting (Ziegel, 2003). To assess the fitness of the models and determine the best model for describing our data, we used the Akaike Information Criterion (AIC; Akaike, 1974) as a common penalized model comparison measure.

The AIC values were calculated based on the natural logarithm of the likelihood function, also known as the log-likelihood. Specifically, the AIC was calculated using the formula:

$$AIC = 2k - 2\ln L,$$

where k represents the number of parameters, and L denotes the maximized value of the likelihood function. At the individual level, we obtained the AIC values using the model comparison function implemented in MemToolbox (Suchow et al., 2013; memtoolbox.org). Lower AIC values indicate a better fit of the model to the data. By subtracting the lowest AIC value (corresponding to the most likely model for each subject) from the AIC values of other models, we obtained the relative AIC values at the subject level.

Additionally, to extend our analysis to the group level, we investigated the model performance against group data. In detail, we first averaged the relative AIC values across all subjects for each experimental condition (e.g., lag). Second, we ranked the models according to their AIC values for each subject and presented the average rankings across all subjects, separately for each condition. This allowed us to gain insights into the overall model performance and make meaningful comparisons among the models within each condition.

2.7. Simulation analysis

Although the AIC indicates how well a model fits the experimental data compared to other models, it does not provide a comprehensive assessment of each model's absolute performance. To gain a more detailed understanding of how well each model captures different aspects of the data, we conducted a simulation analysis. This involved generating simulated data sets from these assessed models and comparing the model predictions to the actual T2 errors in the observed data.

To perform the simulations, we utilized the most probable parameter values from the model fitting procedure described earlier (See *2.5. Model fitting*). These parameters were applied to their respective models for each subject and each condition. We then generated simulated datasets with the same number of data points as those collected from each subject in the corresponding condition. Subsequently, we calculated the summary statistics of T2 errors separately for the simulated data, and the actual data gathered from different studies. This simulation procedure was implemented with a custom-made function in MATLAB, based on the *SampleFromModel* function in Memtoolbox.

2.8. Subject exclusion

The original subject numbers and the final subject numbers in the analysis of each study are listed in Table 1. The subject exclusion based on the Z-scores was carried out to allow more reliable results at the summarized group level. For each study, we calculated the Z-scores for the differences in AIC values between the best model and the worst one for each subject, in each experimental condition. Subsequently, we removed the subjects whose absolute Z-scores exceeded three, as they were considered outliers in the analysis.

3. Results

3.1. Asplund et al. (2014)

3.1.1. Model comparison

Figures 2 and 3 present the model comparison analysis for the Asplund et al. (2014) data. Since Asplund et al.'s data consisted of entirely different T1 and T2 stimuli, the EnsInt model and the Swap model were excluded as they both need a third parameter for the similarity of two targets that was absent here.

Figure 2 shows the results of the T1 correct condition, that is, T2|T1 performance. At the individual level (Figure 2A), the StM, Slot, and SR models consistently exhibited the best fit across most subject's data. The TCC model also showed good fitness for the majority of subjects, although it obtained relatively higher AIC values for a few individuals. As the lag increased, the performance of the StM, Slot, and SR models declined for some subjects, while the performance of the TCC model improved. In terms of the VP model, it consistently showed the poorest performance across almost all subjects, particularly at Lag 1 and 2. Interestingly, the VPG model fitted better than the VP model.

To further assess model performance at the group level, we summarized the individual model fitness values in several ways. First, we calculated the AIC values relative to the best-performing model and then derived their average values across all subjects for each lag (as illustrated in Figure 2B). All models performed commendably across all lags, except for the VPG model, which exhibited larger relative AIC values as the lag decreased. Next, we ranked the models for each subject based on their AIC values and averaged these ranks over all subjects for each lag (Figure 2C). This pattern closely mirrored the model performance depicted in Figure 2B. The StM, Slot, SR and TCC models consistently achieved the lowest ranks (and thus, superior) across all lags. Notably, the TCC model had slightly higher ranks (indicating poorer performance) at Lag 1, but demonstrated improved performance with lower ranks at Lag 2, 4 and 8, in line with its individual level performance. The VPG model, while ranking higher (thus poorer) at Lag 1 and 2, improved its performance at longer lags (Lag 4 and 8). Moreover, the consistency of model performance across different lags indicated that

the AB itself (in particular at Lag 2) did not change the shape of the response error distributions, compared to other lags.

Figure 2

Model comparison for T2 performance when T1 was correct (T2|T1).

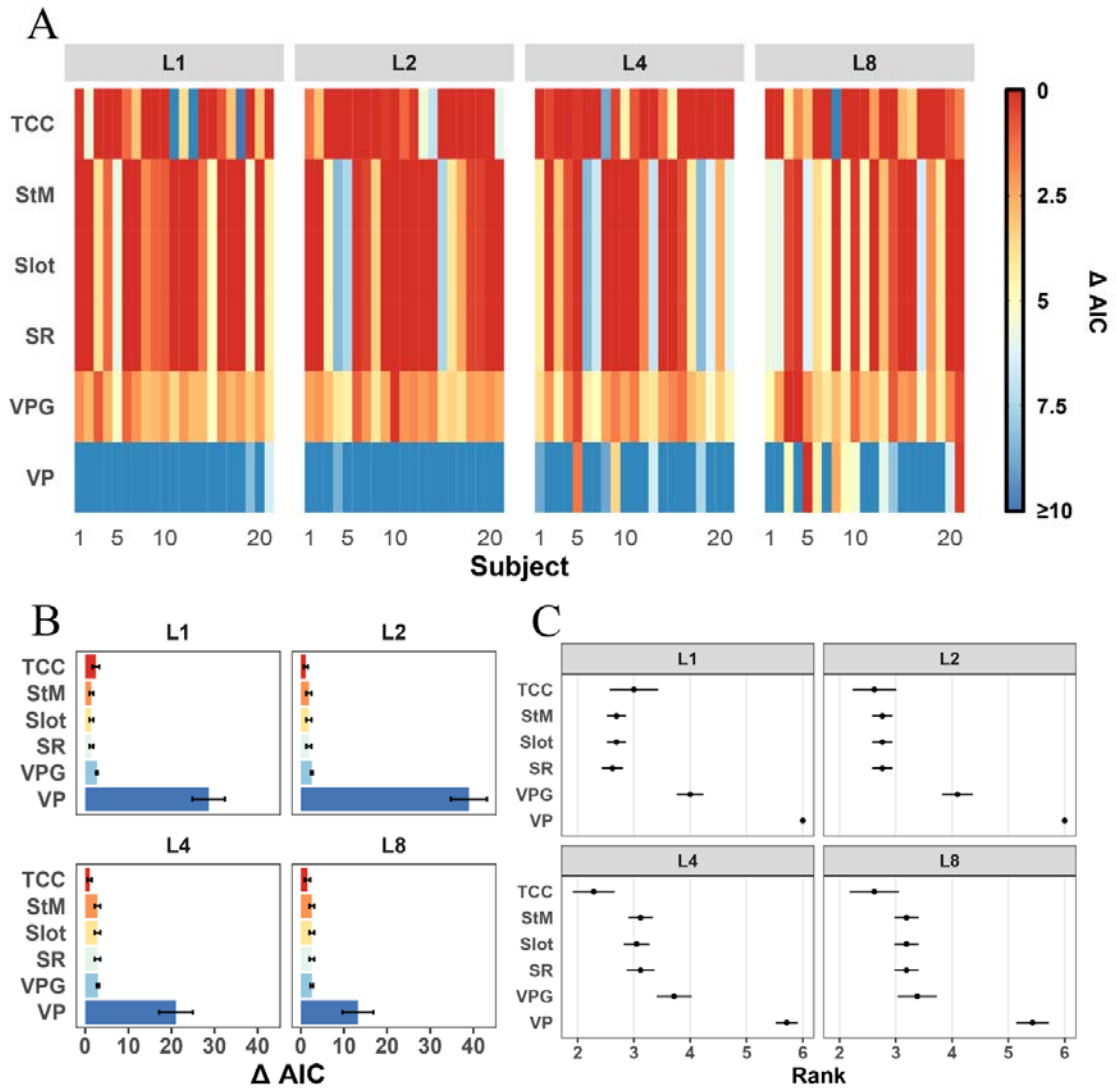

Note. (**A**) Model comparison results at the subject level, using the data from Asplund et al. (2014). Each column represents a subject, and each row represents a specific model. Each panel represents a lag condition. L1 = Lag 1; L2 = Lag 2; L4 = Lag 4; L8 = Lag 8. Cell color indicates each model's relative AIC value. Larger relative AIC values mean worse

performance. (**B**) Relative AIC values compared to that of the best-performing model, averaged across all subjects. Error bars indicate standard error. (**C**) Model ranking. The ranks were obtained by averaging the per-subject ranks for each specific lag. Larger ranks mean worse performance. The model abbreviations are mentioned in the Method (see *2.1. Model details*).

Figure 3 presents the results of model comparison for T2 performance in the T1 incorrect condition. The model comparison pattern bears a resemblance to that in the T1 correct condition, observable at both individual and group levels. Having superior performance across all lags were the TCC, StM, Slot, and SR models. In contrast, the VP model consistently demonstrated poor performance.

Figure 3

Model comparison for T2 performance when T1 was incorrect.

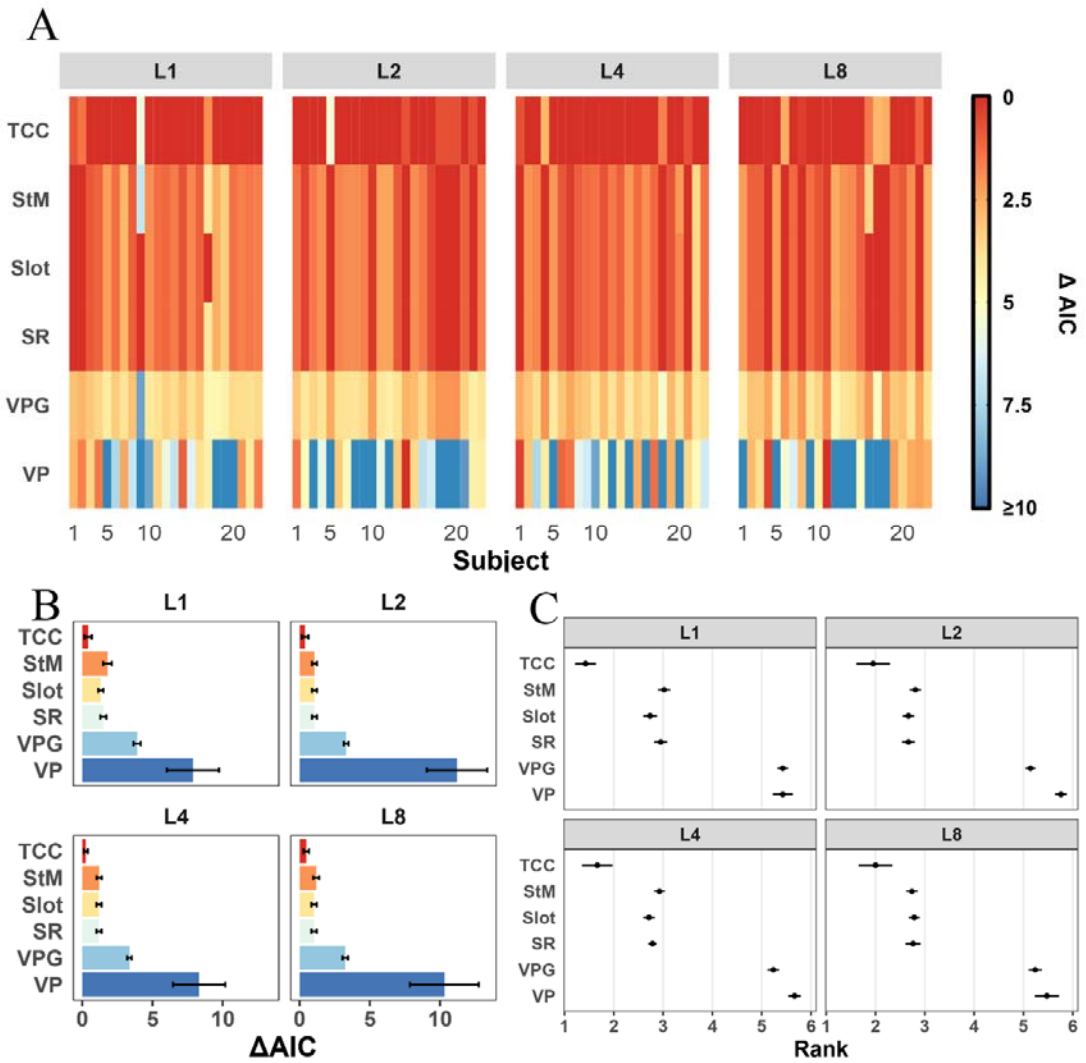

Note. (**A**) Model comparison results at the subject level, using the data from Asplund et al. (2014). (**B**) Relative AIC values, averaged across all subjects for each lag. (**C**) Model ranking at the group level. Figure conventions follow Figure 2.

3.1.2. Simulation analysis

We compared experimentally observed and simulated T2 accuracy for each respective lag. Figure 4 displays the average T2 accuracy across all subjects in both T1 correct and incorrect conditions. Of particular interest was the response error of the second target when the time interval between the first and second target fell between 200 – 500 ms (primarily at Lag 2), to get an idea if these models can actually describe the data well within the AB

window. In general, the pattern of the simulated data was more or less similar to that of the actual data, except for the simulated data obtained from the VP model. One surprising point was that in the T1 correct condition, the SR model estimated relatively high errors. In terms of T2 performance when T1 was incorrect, there was a large divergence between the simulated data of the Slot and VP models and the actual data.

Figure 4

Comparison of model simulations and experimental data based on T2 accuracy.

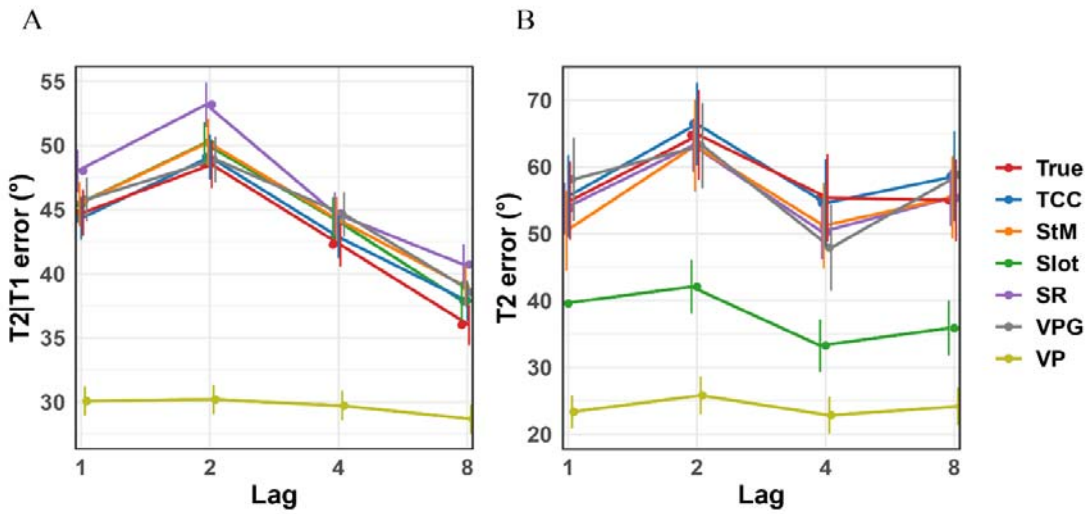

Note. Model simulation results using the data from Asplund et al. (2014). (**A**) Average T2 errors in the T1 correct condition. (**B**) Average T2 errors in the T1 incorrect condition. True = experimentally observed data.

3.2. Tang et al. (2020)

3.2.1. Model comparison[1]

Figure 5 depicts the model comparison results for T2|T1 performance. At the individual level, the TCC, StM, Slot and SR models performed almost identical (Figure 5A).

[1] For the data from Tang et al. (2022), we also conducted further analysis of the Ensemble Integration and Swap models, to investigate the potential interactions between T2 and its subsequent item of T2. Those analyses are presented in the Supplementary Materials (see Supplementary Materials B)

At Lag 1, 2 and 3, these four models showed a good fitness for some individuals, while they behaved poorly for the others (ΔAICs ≥ 16). As lag increased, model performance was improved, and the number of bad individual fits decreased. However, it can clearly be seen that the Swap model consistently showed excellent, if not best, fitness across all subjects and persistently at all lags. It is also worth noting that the number of participants for which the Swap model was the winning one dropped as a function of lag. At Lag 1, 2, and 3, the EnsInt model was the best model for a subset of subjects. The extent of preference for the EnsInt model decreased at Lag 5 and 7, where the EnsInt model showed a relatively consistent and moderate performance across all subjects. The VPG model's performance was only better than its variant, the VP model, for some subjects at short lags (Lag 1, 2, and 3). However, at long lags (Lag 5 and 7), its performance was improved for most subjects. In contrast, the VP model was always the worst fitting one for all subjects at all lags, except for some individuals at Lag 5 and 7. In Experiment 2, there were two lag conditions (Lag 3 and Lag 7). The results presented a similar pattern to Experiment 1 with regard to lag. It was noteworthy that the Swap model was again the winning model for a subset of subjects at Lag 3, but only for two subjects at Lag 7.

The averaged relative AIC values (as displayed in Figure 5B) indicated a lag-dependent change in the models' fitness. During Experiment 1, the TCC, StM, Slot, SR and EnsInt models reached their peak relative AIC values at Lag 2, followed by a decrease at Lag 5 and 7 (refer to Supplementary Materials A for detailed information). The VP and VPG models exhibited a similar pattern. Remarkably, the Swap model consistently registered the smallest ΔAIC values at all lags, maintaining a value of less than 2 points. This finding is coherent with existing AB theories such as the eSTST (Bowman & Wyble, 2007; Wyble et al., 2009), and with the notion of temporal integration (Akyürek & Hommel, 2005). These suggest that targets are bound to same episodic event if they are successively shown, possibly

when the second target is processed (tokenized) more quickly than the first one. Then, timestamps of the targets might be confused, which causes T2 to be reported as T1 and vice versa. For Experiment 2, the Swap model recorded the lowest mean ΔAIC at Lag 3 (1.58), but a slightly higher value (2.36) at Lag 7, at which the StM, Slot and SR models took over the leading positions. Generally, the comparison results from Experiment 2 displayed a similar pattern to that observed in Experiment 1.

The average model ranking at the group level is shown in Figure 5C. For Experiment 1, at Lag 1, 2 and 3, the TCC, StM, Slot, SR, EnsInt and Swap models dominated the top ranks with minimal divergence between them. At Lag 5 and 7, however, the EnsInt and Swap models experienced an increase in ranks (indicating poorer performance) compared to the leading models (the TCC, StM, Slot and SR). The VP and VPG models, on the other hand, consistently ranked last. What stood out in this comparison was the differences in rank across different lags for the EnsInt and Swap models in Experiment 1, a feature not observed in the other models. In Experiment 2, the StM, Slot and SR models achieved the smallest ranks (thus, superior performance) at both Lag 3 and 7.

Figure 5

Model comparison for T2 performance when T1 was correct (T2|T1).

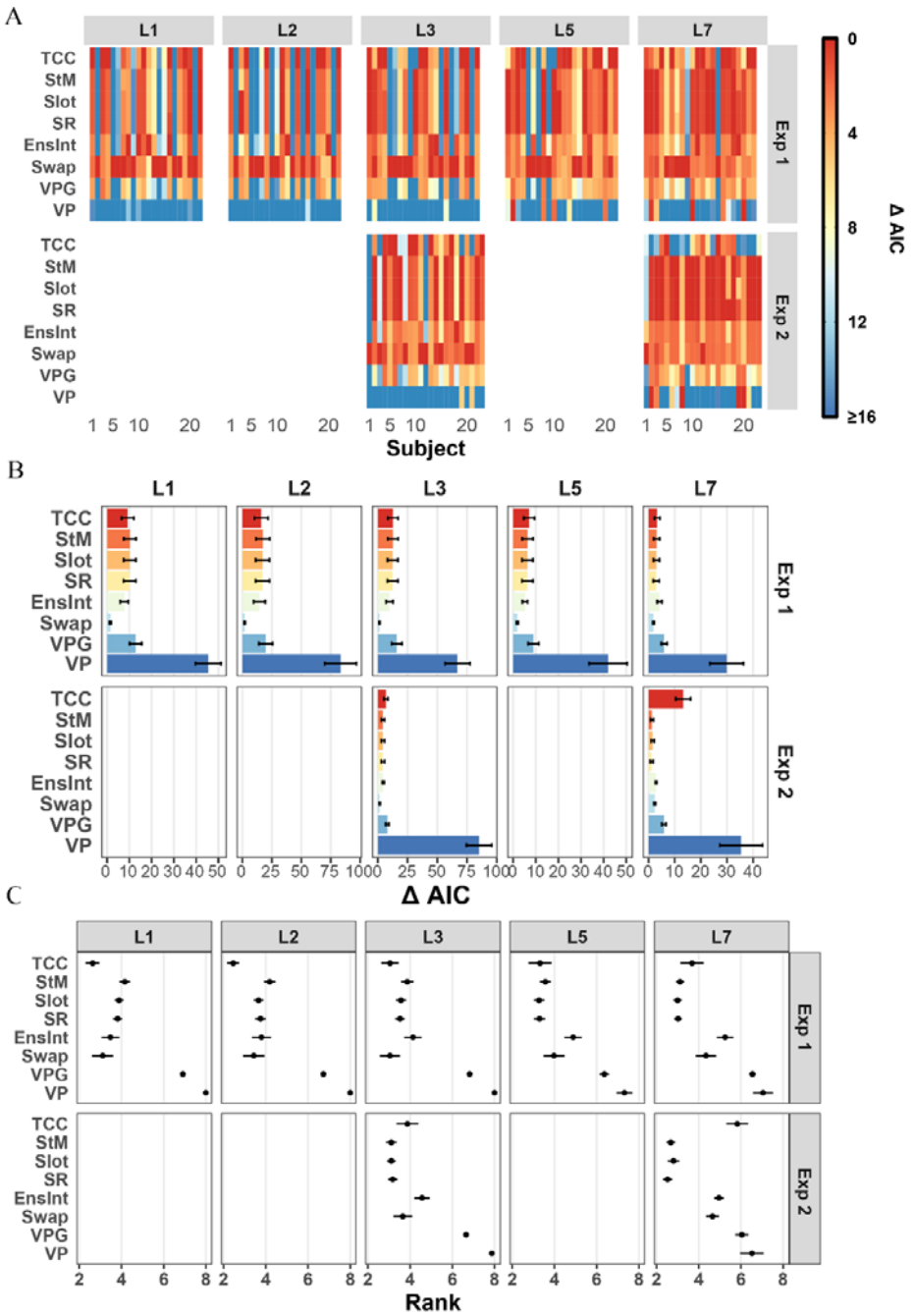

Note. (**A**) Model comparison at the subject level, using the data from Tang et al. (2020). L1 = Lag 1; L2 = Lag 2; L3 = Lag 3; L5 = Lag 5; L7 = Lag7. Exp = Experiment. (**B**) Relative AIC values compared to that of the best-performing model, averaged across all subjects. (**C**) Average model ranking. Figure conventions follow Figure 2.

We observed that when T1 was incorrect, the performance of the models exhibited a more uniform pattern across subjects and lags in both Experiment 1 and Experiment 2. Evidently, the VP model underperformed at both the individual and group level, whereas other models presented either good or moderate fitness. Moreover, the divergences among the top-performing models were fairly minimal.

Figure 6

Model comparison for T2 performance in the T1 incorrect condition.

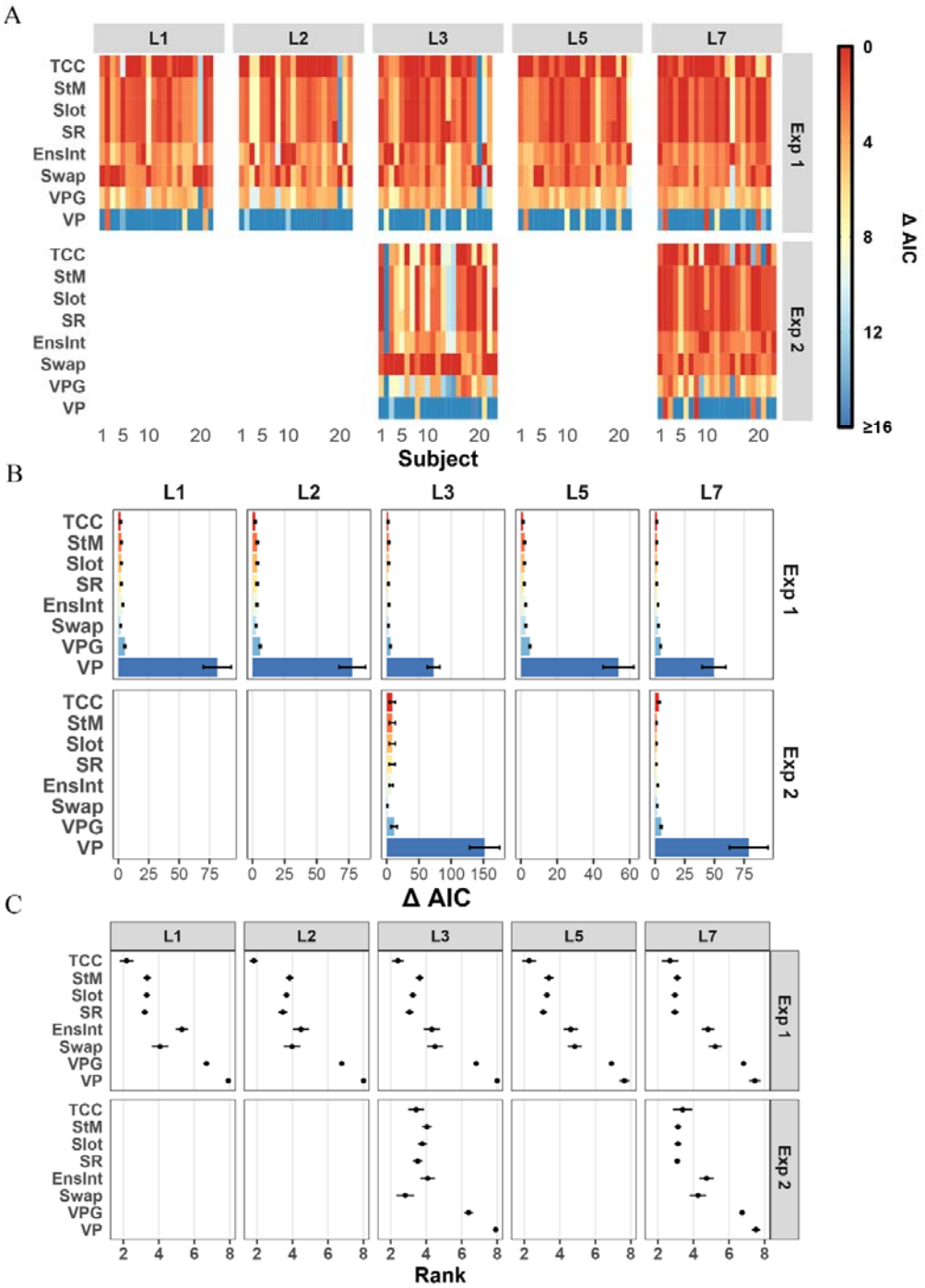

Note. (**A**) Model comparison results at the individual level, using the data from Tang et al. (2020). (**B**) Relative AIC values, averaged across all subjects for each lag and each experiment, respectively. (**C**) Average model ranking. Figure conventions follow Figures 2 and 5.

3.2.2. Simulation analysis

Figure 7 displays the summary statistics for simulated T2 errors from eight models alongside the experimentally observed T2 errors from Tang et al.'s study (2021). It is evident that there was a considerable deviation between the simulated data from the VP model and the other models, compared to the clustering of the simulated data from these latter models around the experimental T2 errors. Although the differences between these models and the experimental data were relatively narrow, a few details are worth noting. First, in Experiment 1, the TCC model generated a distinct T2 response shape, with similar T2|T1 errors at Lag 1 and Lag 2 (Figure 7A), while the True data set exhibited its highest T2|T1 errors at Lag2 (the AB effect). The discrepancy indicates a potential mismatch between the TCC model's simulation and the actual experimental T2 responses. Second, the simulated T2 errors from the Swap model were relatively lower than the corresponding experimental data, particularly in Experiment 1, for both T1 correct and incorrect conditions. This discrepancy suggests that the Swap model may not fully capture certain aspects of the experimental data, leading to lower simulated T2 errors than what was observed in the experiments.

Figure 7

Comparison of model simulations and experimental data based on T2 accuracy.

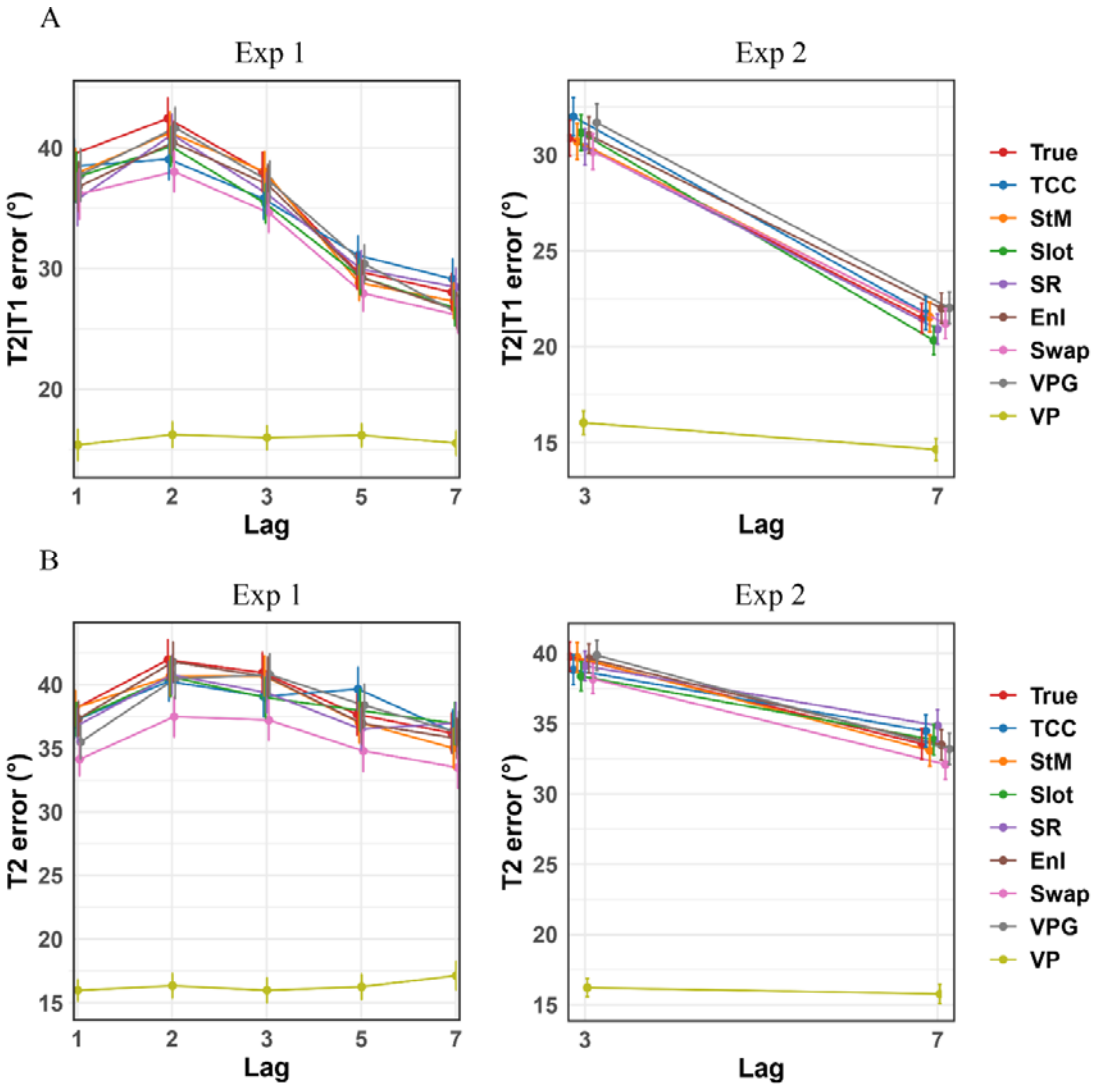

Note. Model simulation results using the data from Tang et al. (2020). Exp = Experiment. (**A**) Average T2 errors in the T1 correct condition. (**B**) Average T2 errors in the T1 incorrect condition. True = experimentally observed data. See Method for model abbreviations.

3.3. Karabay et al. (2022)

3.3.1. Model comparison

Figure 8 presents the model comparison results for T2|T1 performance. When comparing these results across the various experiments within Karabay et al.'s (2022) study,

the most apparent observation was that the models' goodness-of-fit in Experiment 2 was clearly different from those in other experiments, which was evident at both the subject and group level.

Delving into the results at the subject level, in Experiment 2A and 2B, where the targets had only a color feature, the VP and VPG models exhibited a good fit for most subjects at two distinct SOAs. Particularly at long SOA, the VP model outperformed all of its competitors for over half of the subjects. Conversely, the EnsInt and Swap models produced the least accurate data fit, maintaining either relatively higher or the highest ΔAIC values across all subjects. Intriguingly, here the StM, Slot, and SR models showed two extremes of fitness, either being the best or the worst.

In the results of the other experiments, a similar pattern of model fitness is observable. In detail, the StM, Slot, and SR models maintained the lowest ΔAIC values for the majority of subjects; the EnsInt and Swap models had relatively higher ΔAIC values. Additionally, although the VPG model's fitness was the poorest for a subset of subjects, it demonstrated a moderate performance for the others, while the VP model scored the highest ΔAIC values for a majority of individuals.

The performance of the TCC model, however, is complex to interpret. Its performance was inconsistent across all experiments. While it demonstrated good fitness for most subjects under specific conditions (e.g., the short SOA condition in Experiment 1A and 1B and the long SOA condition in Experiment 5), in Experiment 2B and 3, its ΔAIC values were higher (indicating poorer performance) in comparison to the other models for most subjects. For the remaining experiments and conditions, the variations among subjects were pronounced, making it challenging to establish a uniform performance pattern for the TCC model.

In line with the results at the subject level, the VP and VPG models showed superior fitness at the group level in Experiment 2A and 2B, compared to other experiments, as

depicted in Figure 8B. Furthermore, the range of mean ΔAIC values in Experiment 2A and 2B was markedly narrower than those observed in the other experiments. In terms of the model ranking (Figure 8C), the StM, Slot and SR models consistently claimed the leading positions in all experiments, with the exception of Experiment 2A and 2B. It is also worth noting that the EnsInt and Swap models ranked last in these two experiments.

Figure 8

Model comparison for T2 performance when T1 was correct (T2|T1).

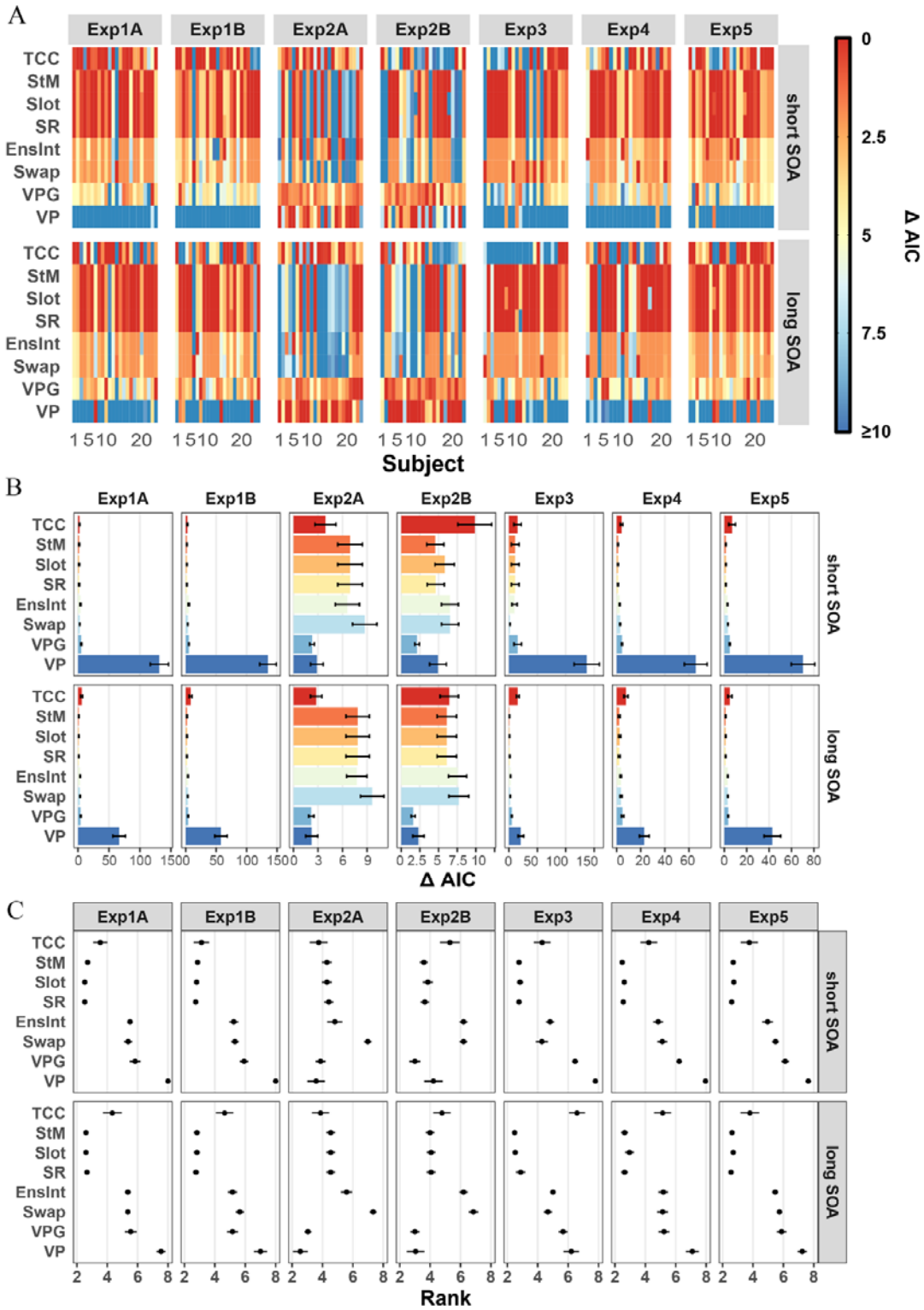

Note. (**A**) Model comparison at the subject level, using the data from Karabay et al. (2022). Exp = Experiment; SOA = stimulus onset asynchrony. (**B**) Relative AIC values compared to

that of the best-performing model, averaged across all subjects. (**C**) Average model ranking. Figure conventions follow Figure 2.

Figure 9 presents the model comparison results for T2 performance when T1 was incorrect. Generally, the models demonstrated a relatively consistent performance across all subjects at the individual level. In addition to this, the pattern of model ranking, as inferred from their averaged ΔAIC values and their average ranks, mostly reflected those observed in the T1 correct condition. Yet, certain differences merit attention in comparison to the T1 correct condition. For example, although the VP and VPG models presented their best fit in Experiment 2A and 2B compared to other experiments, they still occupied the bottom ranks in Experiment 2A and 2B. Also, the TCC model emerged as one of the top-performing models across all experiments. This further indicates subtle variations in model performance in different scenarios.

Figure 9

Model comparison for T2 performance when T1 was incorrect.

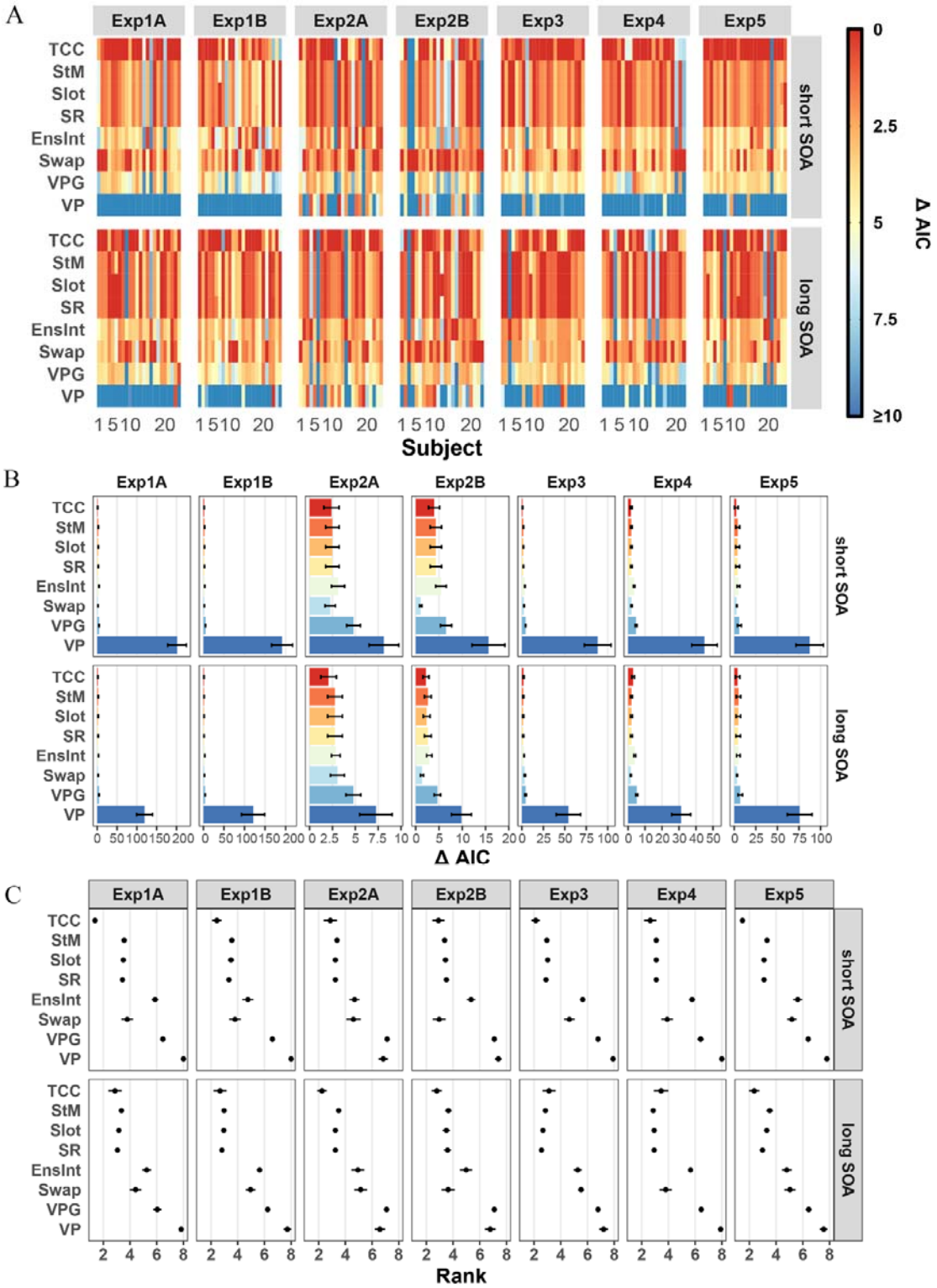

Note. (**A**) Model comparison at the subject level, using the data from Karabay et al. (2022). Exp = Experiment; SOA = stimulus onset asynchrony. (**B**) Relative AIC values compared to

that of the best-performing model, averaged across all subjects. (**C**) Average model ranking. Figure conventions follow Figure 2.

3.3.2. Model Simulation

Figure 10 shows a comparison between the experimental data and the simulated data derived from all eight models. A notable discrepancy was again observed between the VP model and the other seven models. Specifically, the VP model struggled to accurately capture the trend of T2 error across two distinct SOAs (or Lags). However, except for the VP model, the remaining models provided simulations for T2 response errors that were closely aligned with the experimental data, regardless of whether T1 was correct or incorrect. It is worth mentioning that when the targets were colors (in Exp2A and 2B), the VP model's pattern closely mirrored that of the other models.

Figure 10

Comparison of model simulations and experimental data based on T2 accuracy.

A

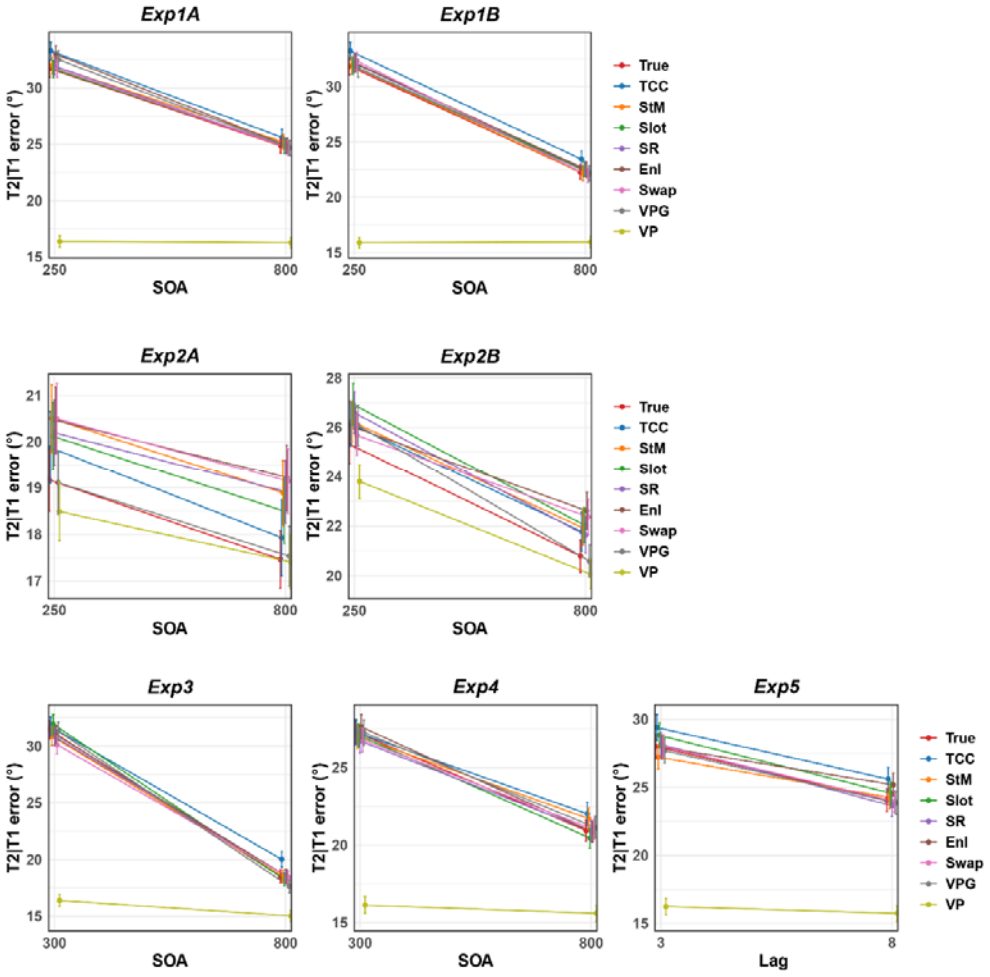

B

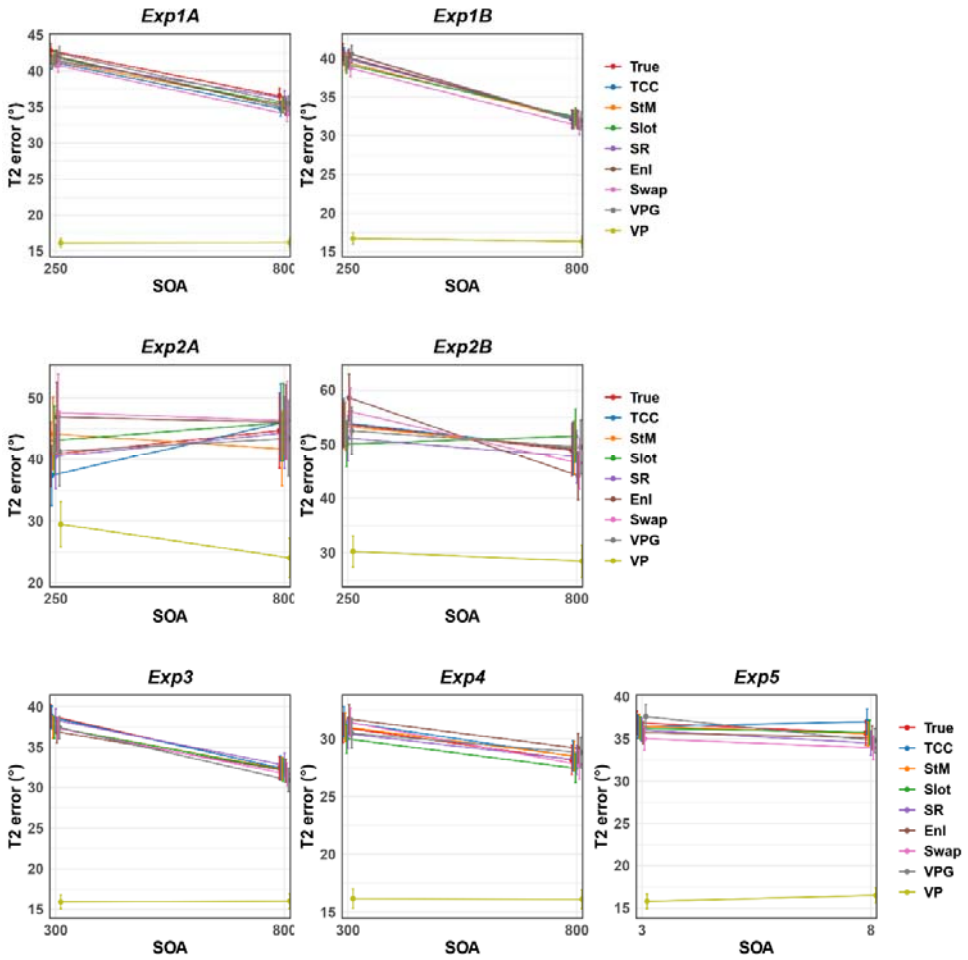

Note. Model simulation results using the data from Karabay et al. (2022). (**A**) Average T2 errors in the T1 correct condition, shown separately for each experiment. (**B**) Average T2 errors in the T1 incorrect condition. Exp = Experiment. True = experimentally observed data. See Method for model abbreviations.

3.4. Wang et al. data

3.4.1. Model comparison

In the model comparison in the T1 correct condition, a standout characteristic of Wang et al.'s data, compared to prior studies, lies in the minimal discrepancies among the candidate models (see Figure 11).

Analyzing at the subject level, we can group these models into three categories based on their performance (Figure 11A). First, the TCC, StM, Slot and SR model consistently demonstrated strong fitness across most subjects under different experimental conditions (lags and target pairs), as indicated by their comparatively lower or the lowest ΔAIC values. Notably, though, the SR model performed poorly for a subset of subjects when the color-color target pair was used. Second, the EnsInt, Swap and VPG models obtained moderate ΔAIC values across most subjects and various conditions, while the EnsInt and Swap models even best fitted several subjects at Lag 1 and 3, when both targets were colors or orientation gratings. Lastly, the VP model exhibited superior and stable performance when the second target was a color item – evident in the color-color and orientation-color target pair conditions. However, its fitness was worse when the second target featured orientation gratings.

The narrow range of mean ΔAIC values for each experimental condition (from 0 to 30; refer to Figure 11B) further underscores the slight variances among models at the subject level. The VP model obviously underperformed when the second target was an orientation grating, as indicated by its highest mean ΔAIC value. Conversely, the VP model exhibited a comparable good fitness when the second target was a colored circle. The VPG, EnsInt and Swap models exhibited relatively inferior fitting across different experimental conditions, as indicated by their higher mean ΔAIC values. Especially for the EnsInt and Swap models, the mean ΔAIC values were higher when the second target was a colored item, as opposed to when the second target was an orientation grating. The average model ranking revealed a nearly identical performance pattern (see Figure 11C). Overall, these feature-dependent model comparison results suggest that the performance of a model is influenced by the stimulus features employed in the experiments.

Figure 11

Model comparison results for T2 performance when T1 was correct (T2|T1).

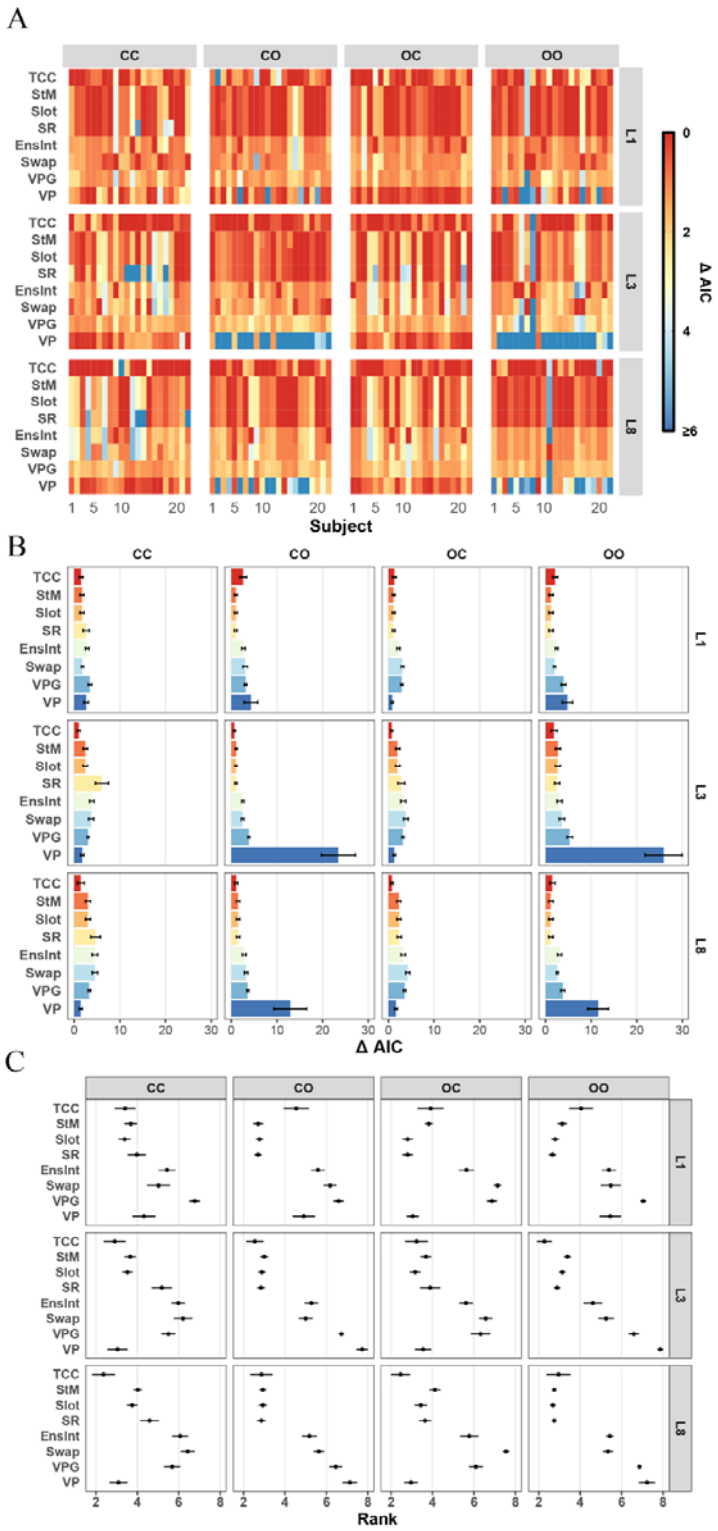

Note. (**A)** Model comparison at the subject level, using the data from Wang et al. The panels in each row present the results with the same lag but different target pairs; the panels in each column present the results with the same target pair but different lags. 'CC' means color-color target pair; 'CO' means color-orientation target pair; 'OC' means orientation-color target pair; 'OO' means orientation-orientation target pair. L1 = Lag 1; L3 = Lag 3; L8 = Lag 8. (**B**) Relative AIC values compared to that of the best-performing model, averaged across all subjects within each condition. (**C**) Average model ranking. Figure conventions follow Figure 2.

Figure 12 illustrates the assessment of these models' fit to T2 data when T1 was incorrect. Because there were insufficient trials for each combination of lag and target pair, we confined our investigation to T2 performance at each lag. Thereby we can still provide an overview of the models' performance in scenarios where only one item was successfully memorized into working memory. The overall pattern was similar to that seen when T1 was correct. For example, the VPG model underperformed compared to the others. Notably, while the Swap model demonstrated superior fitness at Lag 1, these results must be interpreted with caution, due to the combined inclusion of both same- and different-feature target pairs.

Figure 12

Model comparison results for T2 performance when T1 was incorrect.

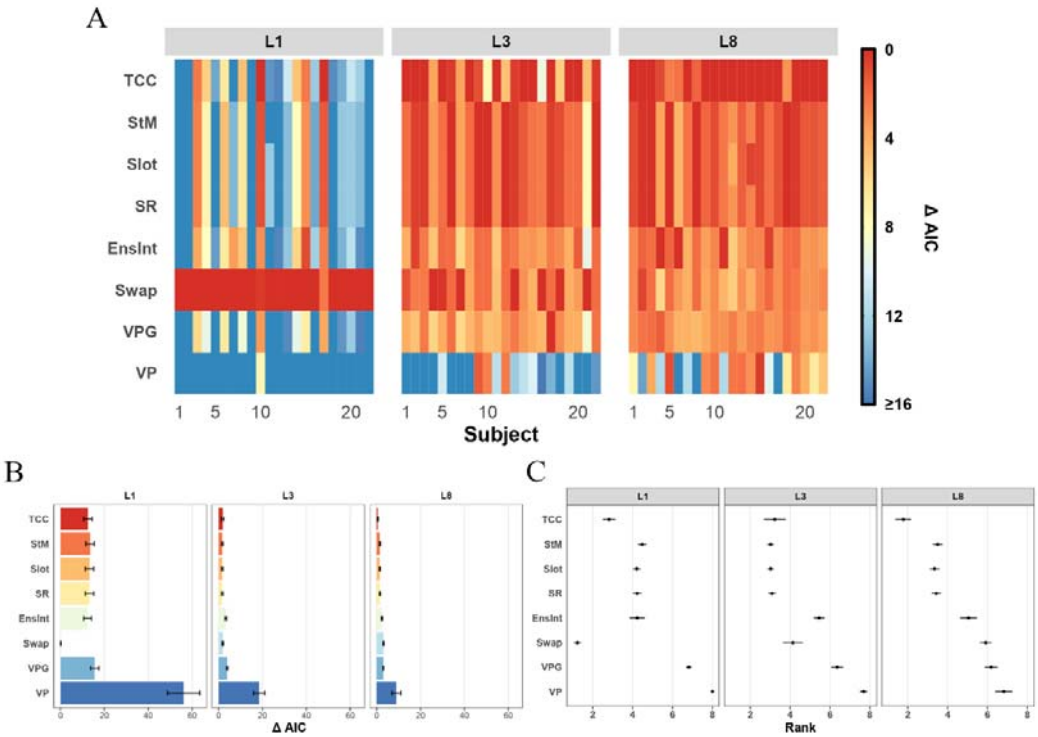

Note. (**A**) Model comparison at the subject level, using the data from Wang et al. L1 = Lag 1; L3 = Lag 3; L8 = Lag 8. (**B**) Relative AIC values compared to that of the best-performing model, averaged across all subjects at each specific lag. (**C**) Average model ranking at each lag. Figure conventions follow Figure 2.

3.4.2. Model Simulation

The results of simulation analysis for the Wang et al. data are depicted in Figure 12. For the T1 correct condition (as shown in Figure 12A), the VPG model did not accurately represent the heightened error at Lag 3 when the second target was an orientation grating. Yet, when the second target was a color, the estimated T2 errors obtained from all models and the actual T2 errors clustered closely. It should be noted that there was no attentional blink detected in the experimental data at Lag 3, when the second target was a color. For the T1 incorrect condition (Figure 12B), a comparison between the simulated and actual data at each lag is possible. Here, the VPG model's estimation of the T2 error was notably less accurate.

Figure 12

Comparison of model simulations and experimental data based on T2 accuracy.

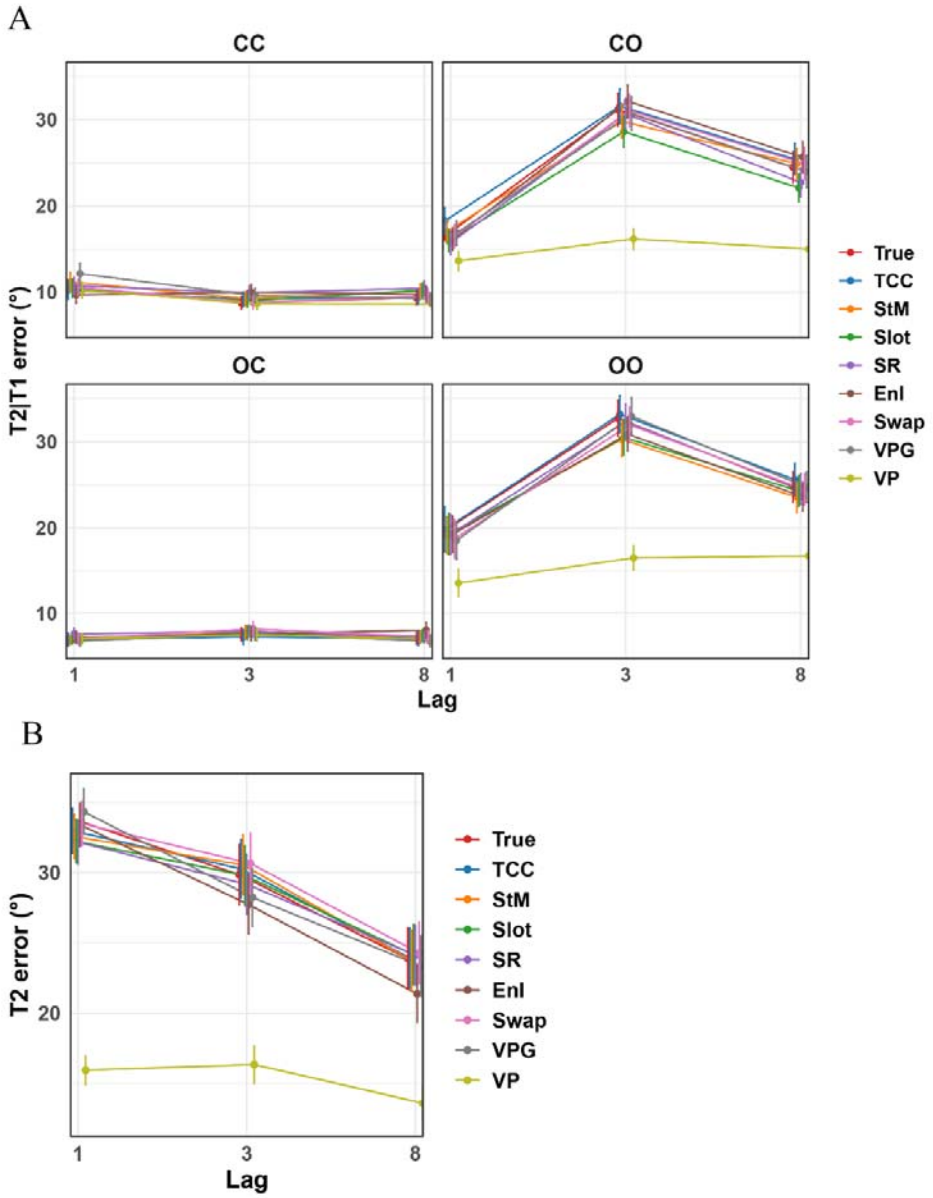

Note. Model simulation results using the data from Wang et al. (**A**) Simulation results in the T1 correct condition. Each panel presents the comparison of the mean T2 error in actual data and in data simulated from eight models, separately for each lag and each target pair condition. 'CC' means color-color target pair; 'CO' means color-orientation target pair; 'OO' means

orientation-orientation target pair; 'OC' means orientation-color target pair. True = experimentally observed data. See Method for model abbreviations. (**B**) Simulation results in the T1 incorrect condition. The results were obtained across all target pairs within each specific lag.

4. Discussion

The current study provided a comprehensive assessment of eight visual WM models, as to their ability to account for continuous reproduction data derived from the AB task. These models have been developed to elucidate the nature of working memory limitations and to offer distinct insights into the explanations for how WM errors occur. There has been substantial research devoted to comparing the performance of these models within the WM field, primarily employing delayed estimation tasks. However, no previous study has systematically compared these models in the AB domain, even though the AB has also been related to limitations in working memory encoding (Akyürek et al., 2007; Jolicœur & Dell'Acqua, 1998; Nieuwenstein et al., 2005; Vul et al., 2008; Wyble et al., 2009; 2011; for a review see also Zivony & Lamy, 2022). Furthermore, models like the EnsInt and Swap, which consider potentially important nontarget reports, have gained little attention in the model selection in the AB domain. Furthermore, the TCC model, which has recently attracted attention in the WM field (Schurgin et al., 2020), has yet to be applied within the AB domain.

Here we therefore attempted to establish which model(s) provide the best account for target representation in the AB task. Specifically, we applied MLE for the parameter estimation, which allowed us to assess model fitness to four data sets of the AB task, from three different laboratories, and then compare them based on the AIC. Moreover, we utilized the parameter values from each model to generate simulated data sets, further probing the

extent to which these models provide an accurate description of the experimental data in all circumstances.

In addressing the central question of this study – which WM model(s) provide a better account of the AB task than others – our findings yielded a clear response: There was substantial evidence, both at the group and subject level, supporting the superiority of the StM, Slot, SR and TCC models across various experiments. Conversely, the EnsInt, Swap, VP, and VPG models generally fell short, with the VP model – assuming no guess rate – underperforming in most conditions. These results align with that of a previous study by Asplund et al. (2014), who also found that the StM model better explains the data from the AB task over the variable precision model families. Three of the leading models, the StM, Slot and SR models share a crucial characteristic, that is, they are based on the hypothesis that not all the items can be encoded into WM, but only a fixed and limited number of items can be stored. In these models' error distributions, when items were not encoded into WM successfully, the corresponding errors obey a uniform distribution indicative of random responses. Intriguingly, even though the TCC model holds a distinct hypothesis compared to the other high-performing models, without the assumption of discrete storage slots in WM, by and large it accounted for the data equally well.

Our study results suggest several reasons as to why the VP and VPG models provided a poorer explanation of the AB task than the others. The simulation analysis unveiled several issues of the VP model: An underestimation of the response errors, and, more specifically, an underestimation of the response errors at shorter lags (SOAs) in relation to longer lags (SOAs), demonstrating a failure to accurately capture impaired memory consolidation during the AB. Contrastingly, the VPG model proved to be better, exhibiting a tendency to align with the empirical data across various conditions. These findings align with the results reported in Experiment 3 of Sy et al. (2021). Given the evident inadequacy of the VP model, especially

compared to its variant that incorporates a guess rate (the VPG model), one might be inclined to conclude that a guess rate component is crucial in accurately predicting WM errors during the AB. For the AB studies tested in the present study, the results provided support for this assertation, with the VP model demonstrating a better performance at longer lags (SOAs), wherein T2 does not suffer from the attentional limitations and can be encoded into WM. Concurrently, the VP model displayed enhanced performance under conditions of a weakened AB, such as in Experiment 2A and 2B of Karabay et al. (2022), as well as with color-color and orientation-color target pairs in the datasets of Wang et al. Our analysis thus suggests that WM errors during the AB are more effectively explained through guessing, as opposed to extremely low precision. This is in keeping with extant literature, which claims that T2 awareness can be discrete during the AB (Asplund et al., 2014; Sy et al., 2021; Wang et al., 2023). However, it is important to note that awareness during the AB can also be gradual, depending on the spatial extent of attention (Karabay et al., 2022), and that the present data also show that the inclusion of a guess rate parameter is not necessary for fitting error distribution during the AB. Our findings also suggest that the TCC model, devoid of extraneous parameters and solely reliant on memory strength, is equally competent in accounting for AB data.

Upon closer examination of the ‘slot’ models (the StM, Slot, and SR models), one might argue that the principal divergence lies in their predictions regarding the number of items that can be successfully encoded into WM, also referred to as set size. This is illustrated by the varying guess rates (P_g) for the Slot and SR models, which are determined based on distinct mathematical calculations that take into account the predicted number of available memory slots. To address this, we expanded our analysis to consider both the T2|T1 performance, indicative of a set size of two, and the T2 performance when T1 was incorrect, indicative of a set size of one. By doing so, we can gain insights into model fitness with

different set sizes. However, we still could not distinguish the performance of the StM, Slot, and SR models at set sizes of 1 and 2 under most conditions. This lack of differentiation could be a consequence of the limited set sizes available in our analyzed data sets (one or two), which are presumably fewer than the number of available visual WM slots as suggested by Cowan (2001). In this case, future research with set size pushing the WM limits will need to be undertaken (e.g., Akyürek et al., 2007).

Our study also investigated the performance of models that consider nontarget reports (the EnsInt and Swap models) in the AB domain. The patterns of performance varied across different scenarios. Specifically, the Swap model's performance appeared to be more influenced by the time interval between the two targets, whereas it was difficult to definitively ascertain whether the EnsInt model's fitness was impacted by different time intervals. For instance, the Swap model performed better at shorter lags, as evidenced in the model comparison results of Tang et al.'s datasets (see Figure 5 and 6), in the single-stream RSVP paradigm of Karabay et al.'s study (e.g., Experiment 3), and also in the same target feature pairs (e.g., color-color and orientation-orientation) of Wang et al.'s data. These results were in accordance with previous research indicating that temporal target integration and target report order reversals occur frequently at Lag 1 (Akyürek et al., 2012; Karabay & Akyürek, 2019). This, in turn, supports the explanation for Lag 1 sparing (i.e., the lack of an AB at that lag) that is offered by the eSTST model of the AB (Wyble et al., 2009), which holds that both targets are consolidated together when they successively follow each other without intervening distractors. This is particularly relevant in AB tasks where both targets share a common feature, as the Swap model's prediction of the T2 error distribution can be influenced by the first target. It might thus be reasonable to conclude that the failure of the Swap model at longer lags could be attributed to the weaker influence of T1 on T2 during memory consolidation. Moreover, when analyzing different set sizes, the Swap model

displayed better fitness when the set size was one (T1 incorrect condition) compared to its performance when the set size was two (T1 correct condition), as noted in the datasets from Karabay et al. and Wang et al. This is likely due to the swap errors at short lags or SOAs, which result in a better performance of the Swap model when T1 is incorrect. Overall, our findings underscore the importance of considering the possibility of swap errors when modelling the error distribution during the AB, especially at shorter lags and when targets share common features.

5. Conclusion

In this study, we embarked on an evaluation of seven well-established and one recent WM models' fitness against for distinct data sets derived from the AB task. Our findings highlight the exceptional performance of models positing a limited number of 'storage slots' in WM. These results suggest that memory errors can be categorized into two distinct types: One representing a complete guess, which occurs when the item was not encoded into WM at all (due to a capacity limitation or processing limitation), and the other representing the precision with which information is encoded into visual WM. This includes the StM, Slot and SR models. Additionally, the recently conceived TCC model also secured a prominent position among these leading models, by predicting working memory representations based on a transformed similarity structure that has a nonlinear relationship with the stimulus space. Overall, it can be argued that all models accounting for the long tails on error distributions fitted well to AB (i.e., the contrast of VPG and VP models). This aligns with the theoretical AB models proposing no conscious access to T2 during the AB (e.g., Asplund et al., 2014; Wyble et al., 2009). Therefore, theoretical reasoning should be as important as the fits in the model choice for AB.

We also identified that the lag between targets, the common features shared by targets, and the nature of the target feature (color or orientation) played an important role in model performance. This underscores the influence of task conditions on the utility of different models, highlighting the need for careful consideration when selecting a model for a given experimental context. If a research question is centered around the short lags (lag 1-3), the EnsInt and Swap models should be preferred. Indeed, a model allowing both swaps and ensemble integrations should be considered for the short lags. However, models without target interactions should be preferred for later lags (lag 4-8; but see Tong et al., 2020). Finally, in our simulation analysis, while there were minor divergences among the synthetic data sets from the models, the VPG model displayed a notably poorer estimation compared to others. In general, our results generally underscore the applicability of these WM models in the AB domain, and offer a roadmap for future model selection in the AB field, which may help to optimize how we assess representation and task performance therein.

Declarations

Acknowledgements We would like to thank Christopher L. Asplund for providing the original data sets from Asplund et al. (2014).

Funding Shuyao Wang was supported by the China Scholarship Council (CSC), grant 201906020179.

Data availability Data generated during the study (Wang et al. data sets), and all the analysis scripts are available on the Open Science Framework at: https://osf.io/zak5f/. The study was not preregistered. The data from Tang et al. (2020) and Karabay et al. (2022) are publicly

available through their published articles. The Tang et al. (202) data can be accessed at: https://osf.io/f9g6h. The Karabay et al. (2022) data can be accessed at: https://osf.io/x5dru.

Conflict of interest The authors have no conflict of interest to disclose.

References

Akyürek, E. G., Eshuis, S. A. H., Nieuwenstein, M. R., Saija, J. D., Başkent, D., & Hommel, B. (2012). Temporal target integration underlies performance at Lag 1 in the attentional blink. *Journal of Experimental Psychology: Human Perception and Performance*, *38*(6), 1448–1464. https://doi.org/10.1037/a0027610

Akyürek, E. G., & Hommel, B. (2005). Target integration and the attentional blink. *Acta Psychologica*, *119*(3), 305–314. https://doi.org/10.1016/j.actpsy.2005.02.006

Akyürek, E. G., Hommel, B., & Jolicœur, P. (2007). Direct evidence for a role of working memory in the attentional blink. *Memory & Cognition*, *35*(4), 621–627. https://doi.org/10.3758/BF03193300

Alvarez, G. A., & Cavanagh, P. (2004). The capacity of visual short-term memory is set both by visual information load and by number of objects. *Psychological Science*, *15*(2), 106–111. https://doi.org/10.1111/J.0963-7214.2004.01502006.X

Asplund, C. L., Fougnie, D., Zughni, S., Martin, J. W., & Marois, R. (2014). The attentional blink reveals the probabilistic nature of discrete conscious perception. *Psychological Science*, *25*(3), 824–831. https://doi.org/10.1177/0956797613513810

Awh, E., Barton, B., & Vogel, E. K. (2007). Visual working memory represents a fixed number of items regardless of complexity. *Psychological Science*, *18*(7), 622–628. https://doi.org/10.1111/j.1467-9280.2007.01949.x

Bae, G. Y., Olkkonen, M., Allred, S. R., Wilson, C., & Flombaum, J. I. (2014). Stimulus-specific variability in color working memory with delayed estimation. *Journal of Vision*, *14*(4), 7–7. https://doi.org/10.1167/14.4.7

Bays, P. M., Catalao, R. F. G., & Husain, M. (2009). The precision of visual working memory is set by allocation of a shared resource. *Journal of Vision*, *9*(10), 1–11. https://doi.org/10.1167/9.10.7

Bonnel, A. M., & Miller, J. (1994). Attentional effects on concurrent psychophysical discriminations: Investigations of a sample-size model. *Perception & Psychophysics*, *55*(2), 162–179. https://doi.org/10.3758/BF03211664

Bowman, H., & Wyble, B. (2007). The simultaneous type, serial token model of temporal attention and working memory. *Psychological Review*, *114*(1), 38–70. https://doi.org/10.1037/0033-295X.114.1.38

Brady, T. F., & Alvarez, G. A. (2011). Hierarchical encoding in visual working memory: Ensemble statistics bias memory for individual items. *Psychological Science*, *22*(3), 384–392. https://doi.org/10.1177/0956797610397956

Broadbent, D. E., & Broadbent, M. H. P. (1987). From detection to identification: Response to multiple targets in rapid serial visual presentation. *Perception & Psychophysics 1987 42:2*, *42*(2), 105–113. https://doi.org/10.3758/BF03210498

Chunharas, C., Rademaker, R. L., Brady, T. F., & Serences, J. T. (2022). An adaptive perspective on visual working memory distortions. *Journal of Experimental Psychology: General*, *151*(10), 2300–2323. https://doi.org/10.1037/xge0001191

Cowan, N. (2001). The magical number 4 in short-term memory: A reconsideration of mental storage capacity. *Behavioral and Brain Sciences*, *24*(1), 87–114. https://doi.org/10.1017/S0140525X01003922

Donkin, C., Nosofsky, R. M., Gold, J. M., & Shiffrin, R. M. (2013). Discrete-slots models of visual working-memory response times. *Psychological Review*, *120*(4), 873–902. https://doi.org/10.1037/a0034247

Dux, P. E., & Marois, R. (2009). The attentional blink: A review of data and theory. *Attention, Perception, & Psychophysics*, *71*(8), 1683–1700. https://doi.org/10.3758/APP.71.8.1683

Faul, F., Erdfelder, E., Lang, A. G., & Buchner, A. (2007). G*Power 3: A flexible statistical power analysis program for the social, behavioral, and biomedical sciences. *Behavior Research Methods*, *39*(2), 175–191. https://doi.org/10.3758/BF03193146

Fougnie, D., & Alvarez, G. A. (2011). Object features fail independently in visual working memory: Evidence for a probabilistic feature-store model. *Journal of Vision*, *11*(12), 1–12. https://doi.org/10.1167/11.12.1

Fougnie, D., Suchow, J. W., & Alvarez, G. A. (2012). Variability in the quality of visual working memory. *Nature Communications*, *3*(1), 1–8. https://doi.org/10.1038/ncomms2237

Jolicœur, P., & Dell'Acqua, R. (1998). The demonstration of short-term consolidation. *Cognitive Psychology*, *36*(2), 138–202.https://doi.org/10.1006/cogp.1998.0684

Karabay, A., & Akyürek, E. G. (2019). Temporal integration and attentional selection of color and contrast target pairs in rapid serial visual presentation. *Acta Psychologica*, *196*, 56–69. https://doi.org/10.1016/j.actpsy.2019.04.002

Karabay, A., Wilhelm, S. A., de Jong, J., Wang, J., Martens, S., & Akyürek, E. G. (2022). Two faces of perceptual awareness during the attentional blink: Gradual and discrete. *Journal of Experimental Psychology: General*, *151*(7), 1520–1541. https://doi.org/10.1037/xge0001156

Kool, W., Conway, A. R. A., & Turk-Browne, N. B. (2014). Sequential dynamics in visual short-term memory. *Attention, Perception, & Psychophysics*, *76*(7), 1885–1901. https://doi.org/10.3758/s13414-014-0755-7

Luck, S. J., Hillyard, S. A., Mouloua, M., & Hawkins, H. L. (1996). Mechanisms of visual-spatial attention: Resource allocation or uncertainty reduction? *Journal of Experimental Psychology. Human Perception and Performance*, *22*(3), 725–737. https://doi.org/10.1037//0096-1523.22.3.725

Luck, S. J., & Vogel, E. K. (1997). The capacity of visual working memory for features and conjunctions. *Nature*, *390*(6657), 279–284. https://doi.org/10.1038/36846

Martens, S., & Wyble, B. (2010). The attentional blink: Past, present, and future of a blind spot in perceptual awareness. *Neuroscience & Biobehavioral Reviews*, *34*(6), 947–957. https://doi.org/10.1016/j.neubiorev.2009.12.005

Mathôt, S., Schreij, D., & Theeuwes, J. (2012). OpenSesame: An open-source, graphical experiment builder for the social sciences. *Behavior Research Methods*, *44*(2), 314–324. https://doi.org/10.3758/S13428-011-0168-7

Miller, G. A. (1956). The magical number seven, plus or minus two: Some limits on our capacity for processing information. *Psychological Review*, *63*(2), 81–97. https://doi.org/10.1037/h0043158

Nieuwenstein, M. R., Chun, M. M., van der Lubbe, R. H., & Hooge, I. T. (2005). Delayed attentional engagement in the attentional blink. *Journal of Experimental Psychology: Human Perception and Performance*, *31*(6), 1463. https://doi.org/10.1037/0096-1523.31.6.1463

Oberauer, K. (2021). Measurement models for visual working memory—A factorial model comparison. *Psychological Review*, *130*(3), 841-852. https://doi.org/10.1037/rev0000328

Oberauer, K., Lewandowsky, S., Farrell, S., Jarrold, C., & Greaves, M. (2012). Modeling working memory: An interference model of complex span. *Psychonomic Bulletin & Review*, *19*(5), 779–819. https://doi.org/10.3758/S13423-012-0272-4

Oberauer, K., Stoneking, C., Wabersich, D., & Lin, H. Y. (2017). Hierarchical Bayesian measurement models for continuous reproduction of visual features from working memory. *Journal of Vision*, *17*(5), 1–27. https://doi.org/10.1167/17.5.11

Pashler, H. (1988). Familiarity and visual change detection. *Perception & Psychophysics, 44*, 369–378. https://doi.org/10.3758/BF03210419

Peirce, J. W. (2007). PsychoPy-Psychophysics software in Python. *Journal of Neuroscience Methods*, *162*(1–2), 8–13. https://doi.org/10.1016/j.jneumeth.2006.11.017

Peirce, J. W. (2009). Generating stimuli for neuroscience using PsychoPy. *Frontiers in Neuroinformatics*, *2*(JAN), 10. https://doi.org/10.3389/neuro.11.010.2008

Potter, M. C., & Levy, E. I. (1969). Recognition memory for a rapid sequence of pictures. *Journal of Experimental Psychology*, *81*(1), 10–15. https://doi.org/10.1037/h0027470

Raymond, J. E., Shapiro, K. L., & Arnell, K. M. (1992). Temporary suppression of visual processing in an RSVP task: An attentional blink? *Journal of Experimental Psychology. Human Perception and Performance*, *18*(3), 849–860. https://doi.org/10.1037//0096-1523.18.3.849

Ricker, T. J., & Hardman, K. O. (2017). The nature of short-term consolidation in visual working memory. *Journal of Experimental Psychology: General*, *146*(11), 1551–1573.https://doi.org/10.1037/xge0000346

Ricker, T. J., Spiegel, L. R., & Cowan, N. (2014). Time-based loss in visual short-term memory is from trace decay, not temporal distinctiveness. *Journal of Experimental Psychology: Learning, Memory, and Cognition*, *40*(6), 1510–1523. https://doi.org/10.1037/xlm0000018

Schmidt, B. K., Vogel, E. K., Woodman, G. F., & Luck, S. J. (2002). Voluntary and automatic attentional control of visual working memory. *Perception & Psychophysics*, *64*(5), 754–763. https://doi.org/10.3758/BF03194742

Schurgin, M. W., Wixted, J. T., & Brady, T. F. (2020). Psychophysical scaling reveals a unified theory of visual memory strength. *Nature Human Behaviour*, *4*(11), 1156-1172. https://doi-org/10.1038/s41562-020-00938-0

Schwarz, G. (1978). Estimating the dimension of a model. *The Annals of Statistics*, *6*(2), 461–464. https://doi.org/10.2307/2958889

Suchow, J. W., Brady, T. F., Fougnie, D., & Alvarez, G. A. (2013). Modeling visual working memory with the MemToolbox. *Journal of Vision*, *13*(10), 9–9. https://doi.org/10.1167/13.10.9

Sy, J. L., Miao, H.-Y., Marois, R., & Tong, F. (2021). Conscious perception can be both graded and discrete. *Journal of Experimental Psychology: General*, *150* (8), 1461. https://doi.org/10.1037/xge0001009

Tang, M. F., Ford, L., Arabzadeh, E., Enns, J. T., Visser, T. A. W., & Mattingley, J. B. (2020). Neural dynamics of the attentional blink revealed by encoding orientation selectivity during rapid visual presentation. *Nature Communications*, *11*(1), 1–14. https://doi.org/10.1038/s41467-019-14107-z

van den Berg, R., Awh, E., & Ma, W. J. (2014). Factorial comparison of working memory models. *Psychological Review*, *121*(1), 124–149. https://doi.org/10.1037/a0035234

van den Berg, R., & Ma, W. J. (2018). A resource-rational theory of set size effects in human visual working memory. *eLife*, *7*. https://doi.org/10.7554/ELIFE.34963

van den Berg, R., Shin, H., Chou, W. C., George, R., & Ma, W. J. (2012). Variability in encoding precision accounts for visual short-term memory limitations. *Proceedings of the National Academy of Sciences of the United States of America*, *109*(22), 8780–8785. https://doi.org/10.1073/pnas.1117465109

Vul, E., Nieuwenstein, M., & Kanwisher, N. (2008). Temporal selection is suppressed, delayed, and diffused during the attentional blink. *Psychological Science*, *19*(1), 55–61. https://doi.org/10.1111/j.1467-9280.2008.02046.x

Wilken, P., & Ma, W. J. (2004). A detection theory account of change detection. *Journal of Vision*, *4*(12), 11–11. https://doi.org/10.1167/4.12.11

Wyble, B., Bowman, H., & Nieuwenstein, M. (2009). The attentional blink provides episodic distinctiveness: Sparing at a cost. *Journal of Experimental Psychology: Human Perception and Performance*, *35*(3), 787–807. https://doi.org/10.1037/A0013902

Wyble, B., Potter, M. C., Bowman, H., & Nieuwenstein, M. (2011). Attentional episodes in visual perception. *Journal of Experimental Psychology: General*, *140*(3), 488–505. https://doi.org/10.1037/a0023612

Zhang, W., & Luck, S. J. (2008). Discrete fixed-resolution representations in visual working memory. *Nature*, *453*(7192), 233–235. https://doi.org/10.1038/nature06860

Ziegel, E. R. (2003). The Elements of Statistical Learning. *Technometrics*, *45*(3), 267–268. https://doi.org/10.1198/tech.2003.s770

Zivony, A., Lamy, D. (2022). What processes are disrupted during the attentional blink? An integrative review of event-related potential research. *Psychonomic Bulletin & Review*, *29*, 394–414. https://doi.org/10.3758/s13423-021-01973-2